

# Hydrophobic membranes for ammonia recovery from digestates in microbial electrolysis cells: assessment of different configurations

Míriam Cerrillo<sup>a</sup>, Laura Burgos<sup>a</sup>, Ernesto Serrano-Finetti<sup>b</sup>, Victor Riau<sup>a</sup>, Joan Noguerol<sup>a</sup>, August Bonmati<sup>a\*</sup>.

<sup>a</sup> IRTA. GIRO. ctra. C-59, km 12,1. E-08140 Caldes de Montbui, Barcelona, Spain.

<sup>b</sup> Department of Electronic Engineering, Universitat Politècnica de Catalunya-BarcelonaTech, Castelldefels, Spain.

\* august.bonmati@irta.cat

## ABSTRACT

The combination of hydrophobic membranes and microbial electrolysis cells (MEC) was assessed in two different configurations in order to recover ammonia from anaerobically digested pig slurry. Polytetrafluorethylene (PTFE) hydrophobic membranes were inserted both in an H-type three-chamber cell (MEC-H) and a two-chamber sandwich configuration MEC (MEC-S), both fitted with a cationic exchange membrane (CEM) dividing the anode and cathode compartments. The use of electrochemical techniques such as electrochemical impedance spectroscopy was applied to monitor the increase of the biofilm on the anode, related to the decrease of the charge transfer resistance. When operated in the higher organic loading rate ( $28 \pm 5 \text{ Kg COD m}^{-3} \text{ d}^{-1}$ ) the current density produced in the MEC-H was  $1.40 \pm 0.71 \text{ A m}^{-2}$ , compared to  $0.61 \pm 0.28 \text{ A m}^{-2}$  in the MEC-S. The flux of ammonium through the CEM in the MEC-H was of  $3.4 \pm 1.2 \text{ g N m}^{-2} \text{ h}^{-1}$ . Regarding the recovery of ammonia through the hydrophobic membrane, the flux of ammonia was of 1.5 and 0.7  $\text{g N m}^{-2} \text{ h}^{-1}$  in the MEC-H and MEC-S, respectively, mainly governed by the pH value and the ammonia concentration of the catholyte. The combination of MEC with hydrophobic membranes reveals as a suitable technology for the recovery of ammonia and treatment of high strength wastewater such as livestock manure.

## Keywords

PTFE, livestock manure, nutrient recovery, bioelectrochemical systems, electrochemical impedance spectroscopy

## 29 **1. Introduction**

30 Waste and wastewater management technologies are evolving in the last years from  
31 the waste removal purpose towards the biorefinery concept. Biorefineries can recover  
32 nutrients and other products of interest from energetic crops, organic wastes and other waste  
33 fluxes [1], including sustainable management practices and closed cycle processes whenever  
34 possible. Wastes, whether industrial, domestic, agricultural, or from livestock are a great  
35 opportunity to recover water, energy, nutrients and chemical products, and have a big  
36 potential for application in biorefineries [2,3].

37 Bioelectrochemical Systems (BES) have emerged as a highly versatile technology that  
38 allows joining the treatment of wastewater to the production or recovery of energy carriers  
39 and compounds such as nutrients [4]. These devices take profit of exoelectrogenic  
40 microorganisms in order to catalyse oxidation and/or reduction reactions. There are several  
41 experiences of using BES in combination with other wastewater treatment technologies, such  
42 as anaerobic digestion, to close nutrient cycles or recover resources and energy [5–8]. The  
43 recovery of ammonia from high strengths wastewater (i.e. livestock manure) is one of the  
44 possible applications of BES and big efforts have been made to optimise the process [9,10].  
45 In a circular economy approach, the recovery and reuse of ammonia from wastewater is a  
46 priority over its removal through technologies such as the nitrification-denitrification process  
47 [11]. Ammonia is a key component in fertilizing activities, and its recovery from waste  
48 streams will reduce the demand of ammonium produced by industrial processes.

49 Previous studies have demonstrated the suitability of BES for ammonia removal from  
50 wastewater using cation exchange membranes in dual chamber reactors, to promote the  
51 migration of cations from the anode to the cathode compartment thanks to the electron flux  
52 between both electrodes [12–16]. Several comprehensive and critical reviews have been  
53 published dealing with ammonia removal in BES [9,17,18], showing the great interest that

54 this technology arises. Once ammonia concentrates in the cathode compartment, a subsequent  
55 recovery step is needed [9]. A stripping and absorption unit can be coupled to the cathode  
56 compartment to easily recover the ammonium in an acidic solution [19,20] thanks to the high  
57 pH value promoted in the cathode compartment of a microbial electrolysis cell (MEC), which  
58 favour the volatilisation of ammonia [10,21,22]. However, the stripping step needs continuous  
59 pumping of air, so it is energy consuming; other alternatives must be tested.

60 Recently, hydrophobic membranes made of polypropylene (PP), polyvinylidene  
61 fluoride (PVDF) or polytetrafluoroethylene (PTFE), permeable to gases, are being applied to  
62 ammonia recovery, in the form of flat, tubular, or hollow fibre membranes [23–26]. This  
63 technology has been tested in anaerobic digestion [27–32] or from raw manure [33–37],  
64 among other substrates. Recovery efficiencies of more than 97% have been achieved in these  
65 assays. Ammonia gas dissolved in a waste stream or a substrate can traverse the pores of the  
66 hydrophobic membrane and react with an acidic solution placed on the other side, typically  
67 sulphuric acid, to form ammonium sulphate.

68 Pilot-scale demonstration plants have been reported for the recovery of ammonia from  
69 swine manure [38], poultry litter [35], from a wastewater treatment plant effluent [39], filtered  
70 anaerobic digestion effluent [40], or from rendering condensate wastewater [41]. Finally, full-  
71 scale nitrogen recovery plants based on gas permeable membranes have been implemented at  
72 Yverdon-les-Bains (Switzerland) wastewater treatment plant (WWTP) [42], Münster  
73 (Germany) WWTP [43] and at Wuppertal (Germany) Membrana GmbH (3M) production site  
74 for industrial wastewater treatment [44].

75 Great efforts are being made to understand the main parameters involved in ammonia  
76 transference through hydrophobic membranes and process modelling [25,31,45,46]. Among  
77 the most important issues to be addressed when working with hydrophobic membranes for

78 ammonia recovering are osmotic distillation, pore wetting and membrane fouling. The first  
79 process occurs as a consequence of the differences in vapour pressure between both sides of  
80 the membrane and leads to a continuous dilution of the acidic solution and the decrease in  
81 ammonia concentration [26,32,37]. Pore wetting makes membranes gradually less  
82 hydrophobic, and is one of the difficulties for fully scale this technology to industrial level  
83 [47]. Regarding fouling, it leads to deterioration of flux, an increase in power consumption,  
84 change in membrane hydrophobicity and a decrease in membrane lifespan [48]. New  
85 configurations and materials are being tested in order to improve membrane fouling and  
86 wetting resistance [49–51].

87         The use of these membranes coupled to the ammonium migration in a MEC could  
88 simplify and reduce the energy demand of the recovery step compared to the stripping and  
89 absorption process [52,53]. Furthermore, compared to the use of hydrophobic membranes in  
90 the anaerobic digestion process, the ammonia transference coupled to the MEC will be  
91 improved thanks to the high pH (>9) of the catholyte, that displace the ammonium/ammonia  
92 equilibrium to the last one gaseous species [21]. This way, no alkali addition or aeration  
93 [33,34] will be needed to maintain the driving force for the membrane separation process,  
94 reducing operation costs. Furthermore, the catholyte, which is in contact with the hydrophobic  
95 membrane, is a clean solution, with no organic neither particulate matter, avoiding  
96 membranes fouling.

97         Previous work has demonstrated that gas-permeable hydrophobic membranes can be  
98 successfully employed in a MEC for ammonia recovery from urine [52,54,55] or as a proton  
99 shuttle to improve the MEC performance [56]. New cell configurations have been proposed  
100 in order to up-scaling ammonia recovery MECs [57]. Also Electrochemical Systems (abiotic  
101 anodes) have been extensively employed in combination with hydrophobic membranes in last  
102 years [58–62]. However, there is a lack of studies about the coupling of these systems to

103 anaerobic digestion for the treatment of high strength wastewaters, such as livestock manure.  
104 In addition, system design improvements are needed to increase ammonia recovery in the  
105 acidic solution and simplify the operation of the reactor. The ammonia recovery system may  
106 be integrated in the recirculation loop of the catholyte, as the most used configuration up to  
107 now [52–54,63], or be integrated in the MEC in a three-compartments system. This last  
108 configuration may simplify MEC operation in a future scale-up of the system, reducing the  
109 number of vessels.

110 Finally, it is important to understand the relation between the bioelectrochemical  
111 performance of BES (due to its direct relation with ammonia transport through the CEM, the  
112 higher the current density the higher the ammonia transport) and anode colonisation by  
113 electrode-reducing microorganisms. In this regard, techniques such as cyclic voltammetry  
114 (CV) or electrochemical impedance spectroscopy (EIS) are being used to monitor biofilm  
115 development on bioanodes [64,65].

116 The aim of this study was to assess the recovery of ammonium and organic matter  
117 removal in a lab-scale MEC connected to a hydrophobic membrane system, as a technology  
118 to be applied to the treatment of organic and nitrogen high strength wastewater. The evolution  
119 of the biofilm developed on the anode of the MECs was also analysed through electrochemical  
120 techniques. Two different configurations were compared, (i) the direct integration of the  
121 hydrophobic membrane in the cathode compartment, and (ii) the integration of the  
122 hydrophobic membrane in the recirculation stream of the catholyte.

123

## 124 **2. Materials and methods**

### 125 **2.1 Experimental set-up**

126 Two different configuration MECs were used in the experiments, (i) an H-type 3  
127 chambers MEC (MEC-H), where the hydrophobic membrane was integrated in the cathode

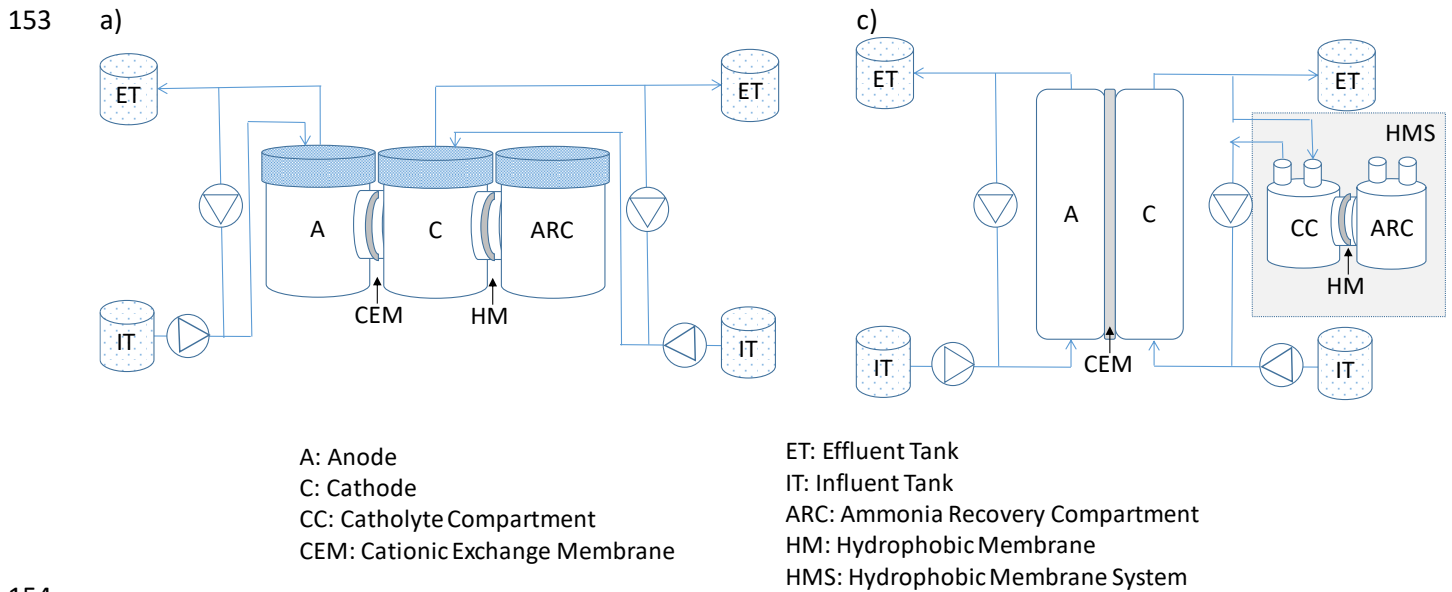
128 compartment; (ii) and a sandwich or flat plate configuration dual-chamber MEC (MEC-S),  
129 where a hydrophobic membrane system (HMS) was integrated in the recirculation stream of  
130 the catholyte.

131 The MEC-H consisted of three 0.6 L glass bottles connected with side openings  
132 (Figure 1a and b). A cation exchange membrane (CEM, dimensions: 20 cm<sup>2</sup>; Ultrex CMI-  
133 7000, Membranes International Inc., Ringwood, NJ, USA) was placed between the side  
134 openings of the first and second (or middle) bottle (anode and cathode compartments,  
135 respectively). A piece of carbon felt (dimensions: 173 cm<sup>2</sup>; thickness: 3.18 mm; Alfa Aesar  
136 GmbH and Co KG, Karlsruhe, Germany) was used as anode; and a 304 stainless steel mesh  
137 was used as cathode (dimensions: 173 cm<sup>2</sup>; mesh width: 150 μm; wire thickness: 112 μm;  
138 Feval Filtros, Spain). A polytetrafluoroethylene (PTFE) flat membrane (0.45 μm pore size,  
139 Filter-Lab) was inserted between the second and third bottle (ammonia recovery  
140 compartment, ARC), achieving a free area of 10 cm<sup>2</sup>. The ARC, where the acidic solution was  
141 placed, was equipped with a magnetic stirrer.

142 The MEC-S was a two-chamber cell (0.5 L each compartment), following the design  
143 described elsewhere [21] (Figure 1c and d). Two different materials were used as anode,  
144 depending on the feeding (i) granular graphite with diameter ranging from 1 to 5 mm (Typ  
145 00514, enViro-cell Umwelttechnik GmbH, Oberursel, Germany), when a synthetic solution  
146 was used as anolyte; (ii) carbon felt (168 cm<sup>2</sup>), with the same characteristics than the MEC-  
147 H, when digestate was used as anolyte. The same stainless-steel cathode and CEM (168 cm<sup>2</sup>  
148 each one) as in the MEC-H was used in the MEC-S. This way, the surface of the MEC-H  
149 CEM represented 12% of the MEC-S CEM, calculated as the ratio between CEM areas,  
150  $CEM_{MEC-H}/CEM_{MEC-S}$ , because of the different system configuration.

151

152



154  
 155

156

157 **Figure 1.** Scheme (a) and picture (b) of the MEC-H, and scheme (c) and picture (d) of the MEC-S with the HMS  
 158 connected.

159

160 For the MEC-S, a hydrophobic membrane system (HMS) was integrated in the  
 161 catholyte recirculation stream to recover the ammonium transferred from the anode to the  
 162 cathode compartment. Two glass bottles (0.25 L each one) with a side opening were  
 163 connected, inserting a PTFE membrane between them as described before (10 cm<sup>2</sup>). One of  
 164 the chambers was filled with catholyte, while the second chamber was filled with an acidic  
 165 solution (H<sub>2</sub>SO<sub>4</sub>, 1.8 M). Both chambers were equipped with a magnetic stirrer.

166 A potentiostat (VSP, Bio-Logic, Grenoble, France) was used to poise the anode  
 167 (working electrode) potential to 0 mV in a three-electrode mode, with an Ag/AgCl reference

168 electrode (Bioanalytical Systems, Inc., USA; +197 mV vs. standard hydrogen electrode, SHE)  
169 inserted in the anode compartment of each cell. All potential values in this paper are referred  
170 to SHE. The potentiostat was connected to a personal computer, which recorded electrode  
171 potentials and current, every 5 min, using EC-Lab software (Bio-Logic, Grenoble, France).

172

## 173 **2.2 Feeding solutions**

174 The MEC-S anode compartment synthetic feeding solution (COD of  $2.2 \text{ g}_{\text{O}_2} \text{ L}^{-1}$  and  $1$   
175  $\text{g}_{\text{NH}_4\text{-N}} \text{ L}^{-1}$ ) contained (per litre of deionized water):  $\text{CH}_3\text{COONa}$ , 2.9 g;  $\text{NH}_4\text{Cl}$ , 0.87 g;  $\text{CaCl}_2$ ,  
176 14.7 mg;  $\text{KH}_2\text{PO}_4$ , 3 g;  $\text{Na}_2\text{HPO}_4$ , 6 g;  $\text{MgSO}_4$ , 0.246 g; and  $1 \text{ mL L}^{-1}$  of a trace elements  
177 solution. The solution of trace mineral contained (per litre of deionized water):  $\text{FeCl}_3 \cdot \text{H}_2\text{O}$ ,  
178 1.50 g;  $\text{H}_3\text{BO}_3$ , 0.15 g;  $\text{CuSO}_4 \cdot 5\text{H}_2\text{O}$ , 0.03 g;  $\text{KI}$ , 0.18 g;  $\text{MnCl}_2 \cdot 4\text{H}_2\text{O}$ , 0.12 g;  
179  $\text{Na}_2\text{MoO}_4 \cdot 2\text{H}_2\text{O}$ , 0.06 g;  $\text{ZnSO}_4 \cdot 7\text{H}_2\text{O}$ , 0.12 g;  $\text{CoCl}_2 \cdot 6\text{H}_2\text{O}$ , 0.15 g;  $\text{NiCl}_2 \cdot 6\text{H}_2\text{O}$ , 0.023 g;  
180 EDTA, 10 g. This composition was chosen to simulate a diluted pig slurry regarding COD,  
181 ammonia content and alkalinity.

182 The digestate used to feed the anode compartment of the MEC-S and the MEC-H was  
183 collected from a lab-scale thermophilic anaerobic digester, which was fed with pig slurry. The  
184 digestate was stored at  $6^\circ \text{C}$  until its use and sieved ( $125 \mu\text{m}$ ). The sieved digestate (pH of  
185  $8.1 \pm 0.2$ , COD of  $21.9 \pm 3.3 \text{ g}_{\text{O}_2} \text{ L}^{-1}$  and  $\text{NH}_4\text{-N}$  of  $1.9 \pm 0.3 \text{ g L}^{-1}$ ) was diluted with tap water to  
186 achieve the different organic loading rates used during the experiment (Table 1).

187 The cathode compartments were fed with a  $\text{NaCl}$   $0.1 \text{ g L}^{-1}$  solution.

188

189

190

191

192



## 193 **2.3 Reactors operation**

### 194 **2.3.1 HMS batch assays**

195 In a first block of experiments, in order to characterise the  $\text{NH}_4^+$ -N flux through the  
196 PTFE membrane, a series of batch assays were performed with the HMS alone, before  
197 connecting it to the MEC-S.

198 The catholyte compartment was filled with a synthetic  $500 \text{ mg L}^{-1} \text{ NH}_4^+$ -N solution at  
199 three different pH values (10, 11 and 12), simulating the composition of the cathode effluent.  
200 This  $\text{NH}_4^+$ -N concentration was chosen as the one expected when the MEC-S was to be fed  
201 with digestate, accordingly to previous work [21]. A lower concentration, of  $125 \text{ mg L}^{-1} \text{ NH}_4^+$ -  
202 N, was also assessed at pH 11 to simulate the conditions expected in the synthetic operation  
203 of the MEC-S. The pH values were adjusted with NaOH to the desired value at the beginning  
204 of the experiment, without any regulation throughout the assay. The acid compartment (ARC)  
205 was filled with  $\text{H}_2\text{SO}_4$ , 1.8 M.

206 Each batch lasted for 48 h, and started filling both compartments with the  
207 corresponding solution and switching on the magnetic stirring. Samples were taken from both  
208 compartments at time 0, 3, 6, 24, 31 and 48 h. Once a batch was finished, the compartments  
209 were emptied and rinsed with deionised water before starting the following one. The different  
210 conditions were tested in triplicate.

211

### 212 **2.3.2 Continuous synthetic fed MEC-S assay**

213 Regarding the MEC-S operation, the anode compartment was inoculated with graphite  
214 granules from the anode of a lab-scale mother MEC operated with synthetic medium  
215 containing acetate. The MEC-S with no HMS inserted was operated for 1.5 years before  
216 starting these assays, so it was considered that the biofilm was mature.

217 The MEC-S with the HMS was operated for 190 days. The influent solutions of both  
218 the anode and the cathode compartments were fed in continuous mode with a pump at 20 mL  
219 h<sup>-1</sup> and mixed by recirculating them by an external pump. The feeding velocity of the cathode  
220 compartment was reduced from day 105 to 14 mL h<sup>-1</sup>, to favour the increase of ammonium  
221 concentration in the catholyte. The hydraulic retention time (HRT) of each compartment was  
222 of 12.6 h, 20.6 h and 10.3 h for the anode, cathode and HMS catholyte compartment,  
223 respectively (with respect to the net volume of each compartment), and the organic loading  
224 rate (OLR) of the anode compartment was established at 7.83 kg<sub>COD</sub> m<sup>-3</sup> day<sup>-1</sup>. These HRT  
225 were increased the last 85 days of operation for the cathode and HMS catholyte compartments  
226 to 36.6 h and 18.3 h, respectively. The acidic solution of the ARC was replaced when it  
227 became saturated with ammonia. Samples of the anode and cathode compartment effluents  
228 and from the ARC were taken on weekdays. The MEC-S was operated at room temperature  
229 during the entire assay (23±2 °C).

230

### 231 **2.3.3 Continuous digestate fed assays**

232 Before starting the operation with digestate, the granular graphite anode of the MEC-  
233 S was replaced with carbon felt to avoid clogging due to suspended solids content of the new  
234 feeding. Both the MEC-S and the MEC-H anodes were inoculated with the anode  
235 compartment effluent from a lab-scale MEC operated with synthetic solution. Both reactors  
236 were operated in continuous with synthetic solution in a start-up period until current density  
237 production stabilized. After 26 days of operation, the influent was switched to diluted digested  
238 pig slurry. The dilution was stepwise decreased, from 3 times diluted digestate (1 L digestate:  
239 2 L water) to undiluted digestate, to adapt the anode biofilms to increasing OLR and nitrogen  
240 loading rate (NLR), accordingly to Table 1. The MECs were operated with digested pig slurry  
241 for 115 days. On day 57, the cathode compartments of both cells were switched from

242 continuous to batch mode operation to improve the conditions for ammonia diffusion through  
 243 the hydrophobic membrane. The acidic solution of the ARC was replaced when it became  
 244 saturated with ammonia, monitoring the solution pH. Sampling of the anode and cathode  
 245 compartments effluents and from the ARCs started after switching to 1.5 diluted digestate,  
 246 and was performed on daily basis. Both MECs were operated at room temperature during the  
 247 entire assay ( $23\pm 2$  °C).

248

249 **Table 1.** Organic (OLR) and nitrogen (NLR) loading rates of the MECs in the different phases of digestate operation.

Phase	Period (d)	OLR ( $\text{Kg}_{\text{COD}} \text{m}^{-3} \text{d}^{-1}$ )	NLR ( $\text{Kg}_{\text{NH}_4^{++}\text{N}} \text{m}^{-3} \text{d}^{-1}$ )
1	0-25	$6\pm 1$	$1.0\pm 0.2$
2	26-36	$9\pm 2$	$1.0\pm 0.2$
3	37-74	$15\pm 2$	$1.5\pm 0.2$
4	75-115	$28\pm 5$	$2.9\pm 0.4$

250

## 251 **2.4. Analytical methods and calculations**

252 Ammonium nitrogen ( $\text{NH}_4^+\text{-N}$ ) and pH were determined in the anolyte and catholyte  
 253 effluent and acidic solution samples. The bulk solution pH in each sample was measured using  
 254 a CRISON 2000 pH electrode (Hach Lanhe Spain, S.L.U., L'Hospitalet de Llobregat, Spain).  
 255  $\text{NH}_4^+\text{-N}$  was analyzed by a Büchi KjelFlex K-360 distiller (Büchi Labortechnik AG, Flawil,  
 256 Switzerland), capture of distillate in boric acid and subsequent titration with 0.1 M HCl with  
 257 a Metrohm 702 SM autotitrator (Metrohm AG, Herisau, Switzerland). Chemical oxygen  
 258 demand (COD) was determined in anolyte feeding and effluent samples. All the analyses were  
 259 performed following Standard Methods [66].

260 The current density ( $\text{A m}^{-2}$  or  $\text{A m}^{-3}$ ) of the MECs was calculated as the quotient  
 261 between the intensity recorded by the potentiostat (A) and the area of the anode ( $\text{m}^2$ ) for MEC-  
 262 S and MEC-H (carbon felt); or the net volume of the anode compartment ( $\text{m}^3$ ) for the MEC-  
 263 S (granular graphite in synthetic operation). Ammonium and COD removal efficiencies in the  
 264 MECs were calculated as the ratio of the difference between the anode compartment influent

265 and effluent concentrations and the influent concentration. Ammonium recovery efficiency  
266 in the acidic solution was calculated as the ratio between the amount of ammonium removed  
267 from the anode compartment in a day and the ammonium accumulated in the acidic solution  
268 in the same period. Regarding batch test, for HMS characterisation, recovery efficiency was  
269 calculated as the ratio between the amount of ammonia found in the acid compartment at the  
270 end of the assay and the initial amount of ammonia in the catholyte compartment. Ammonia  
271 flux through the membranes, expressed in the form of ammonium nitrogen,  $\text{NH}_4^+\text{-N}$ , ( $\text{g N m}^{-2}$   
272  $\text{h}^{-1}$ ) was calculated as the ratio between the amount of ammonium nitrogen transferred (g)  
273 and the elapsed time (h) and the membrane surface ( $\text{m}^2$ ).

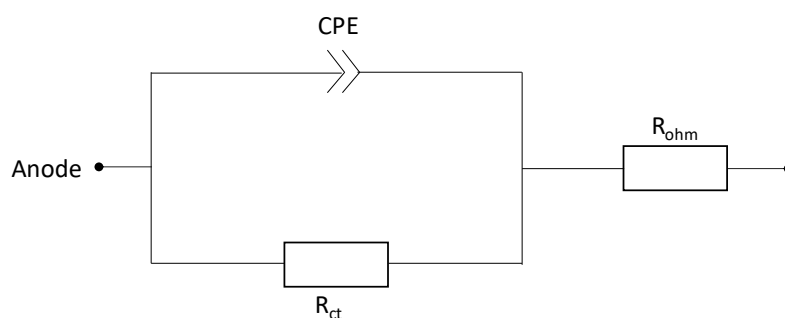
274

## 275 **2.5. Electrochemical measurements**

276 Electrochemical impedance spectroscopy (EIS) measurements and cyclic  
277 voltammeteries (CV) were performed periodically on the MECs to characterise the anodic  
278 biofilm development, on days 0, 20, 26, 36, 56, 69, 77, 90 and 106. Both techniques were  
279 carried out using a potentiostat equipped with an impedance module (VSP, Bio-Logic,  
280 Grenoble, France). EC-Lab software (V11.20, Biologic Science Instruments) was used for  
281 instrument control and data analysis. The measurements were done in a three-electrode mode,  
282 with the same configuration as described in the Experimental set-up Section. EIS test were  
283 performed at an AC signal amplitude of 10 mV, between 100 kHz and 10 mHz. CV was  
284 carried out at a scan rate of  $1 \text{ mV s}^{-1}$ , and with an amplitude between -0.1 and -0.6 V.

285 The Randles equivalent circuit shown in Figure 2 was used to fit EIS data and identify  
286 parameters dominating electrical behaviour at the bioanodes. This equivalent circuit model  
287 consisted of an ohmic resistance component ( $R_{\text{ohm}}$ ), followed by an electrochemical charge  
288 transfer resistance ( $R_{\text{ct}}$ ) in parallel with a double layer constant phase element (CPE). The  
289 CPE is used instead of a capacitor to simulate the non-ideal behaviour of distributed

290 capacitance, typical of porous electrodes [67]. No Warburg diffusion element was included  
291 in the circuit, since no tails related to diffusion phenomena were generally detected.



292

293 **Figure 2.** Equivalent circuit used for the analysis of impedance of the anodic biofilm (CPE, constant phase element;  $R_{ct}$ ,  
294 charge transfer resistance;  $R_{ohm}$ , ohmic resistance).

295

296 EIS data were plotted in Nyquist plots, expressing the real ( $Z_{re}$ ) and the imaginary  
297 impedance ( $Z_{im}$ ) in the horizontal and vertical axis, respectively. The intercept of the curve  
298 with the real impedance ( $Z_{re}$ ) axis at the highest frequencies (left side of the axis) has been  
299 considered as the ohmic resistance ( $R_{ohm}$ ) and the  $Z_{re}$  value of the lowest frequency (where  
300  $Z_{im}=0$ ) has been considered as the total  $R_{int}$  [68]. The magnitude of the Nyquist arc  
301 qualitatively yields the charge-transfer ( $R_{ct}$ ) resistance of the anode.

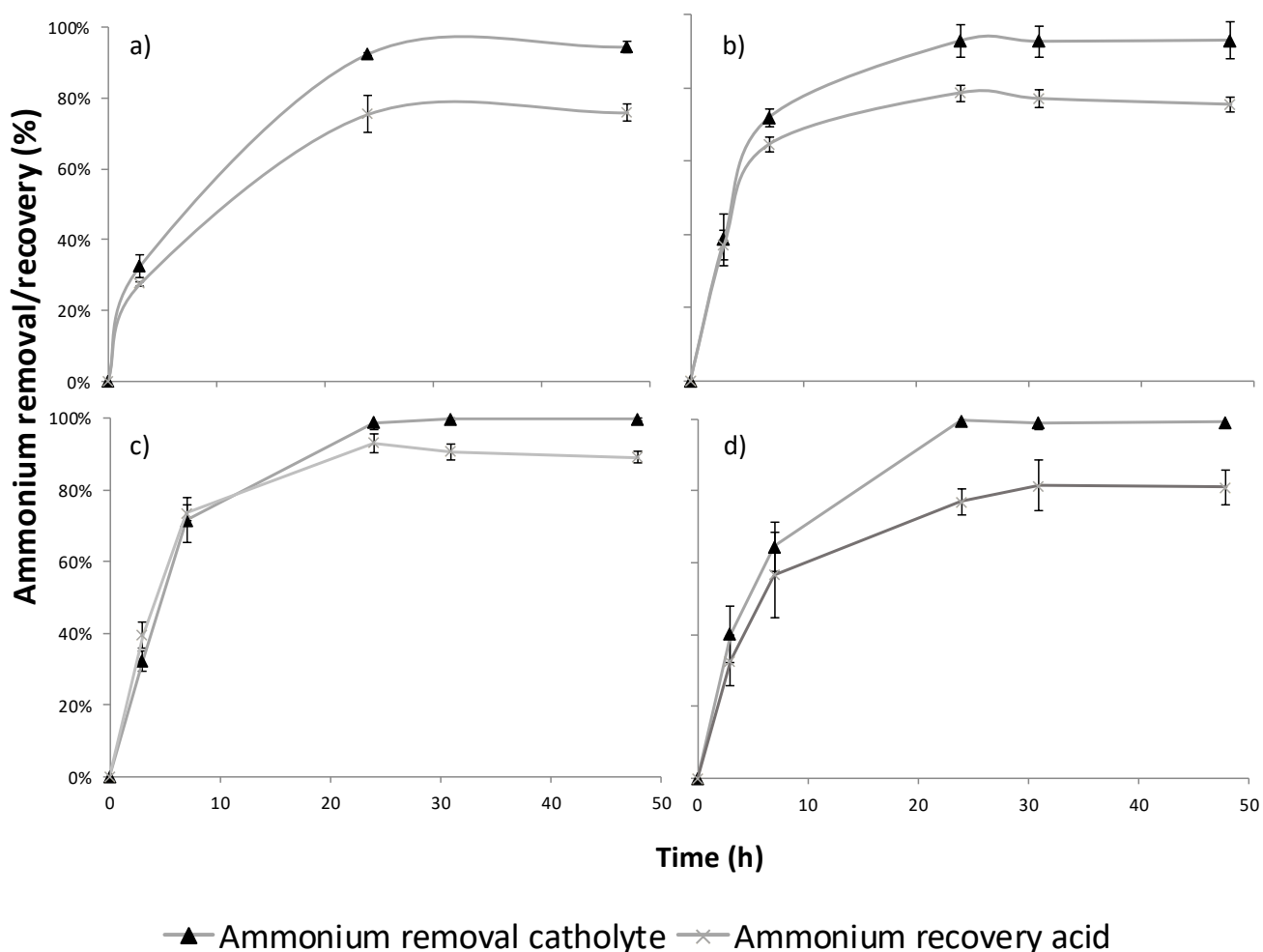
302

### 303 **3. Results and discussion**

#### 304 **3.1. Performance of the HMS**

305 The HMS characterisation (Figure 3) showed that ammonia removal efficiency from  
306 synthetic catholyte in 48 h achieved  $94\pm 2\%$ ,  $93\pm 5\%$  and  $100\pm 1\%$  at pH 10, pH 11 and pH 12,  
307 respectively, when using an initial concentration of  $NH_4^+-N$  of  $500\text{ mg L}^{-1}$ . The efficiency  
308 achieved  $99\pm 1\%$  when using an initial concentration of  $NH_4^+-N$  of  $125\text{ mg L}^{-1}$  with a pH of  
309 11. Although these high removal efficiencies, the recovery efficiencies in the acid  
310 compartment increased with the pH ( $73\pm 3\%$ ,  $75\pm 2\%$  and  $89\pm 2\%$  at pH 10, pH 11 and pH 12,  
311 respectively) but were lower than the removal efficiencies, probably due to ammonia

312 volatilisation phenomena in the catholyte compartment due to the basic pH values. In the case  
 313 of an initial concentration of  $\text{NH}_4^+\text{-N}$  of  $125 \text{ mg L}^{-1}$  with a pH of 11, the recovery efficiency  
 314 was of  $81 \pm 5\%$ , slightly higher than that for the equivalent pH and  $500 \text{ mg L}^{-1}$  initial  
 315 concentration. Ammonia transfer rate through the hydrophobic membrane was of  $12.7 \pm 0.3$ ,  
 316  $13.1 \pm 0.4$ , and  $14.1 \pm 0.4 \text{ g N m}^{-2} \text{ h}^{-1}$  at pH values of 10, 11, and 12, respectively, while it  
 317 decreased to  $3.4 \pm 0.7 \text{ g N m}^{-2} \text{ h}^{-1}$  with the initial concentration of  $125 \text{ mg L}^{-1}$  with a pH of 11.  
 318 The obtained results agree with the observations of other studies, which reported an increase  
 319 in ammonia flux through tubular gas permeable membranes when increasing pH or  
 320 ammonium concentration of the substrate [25,30,49,69,70].



321

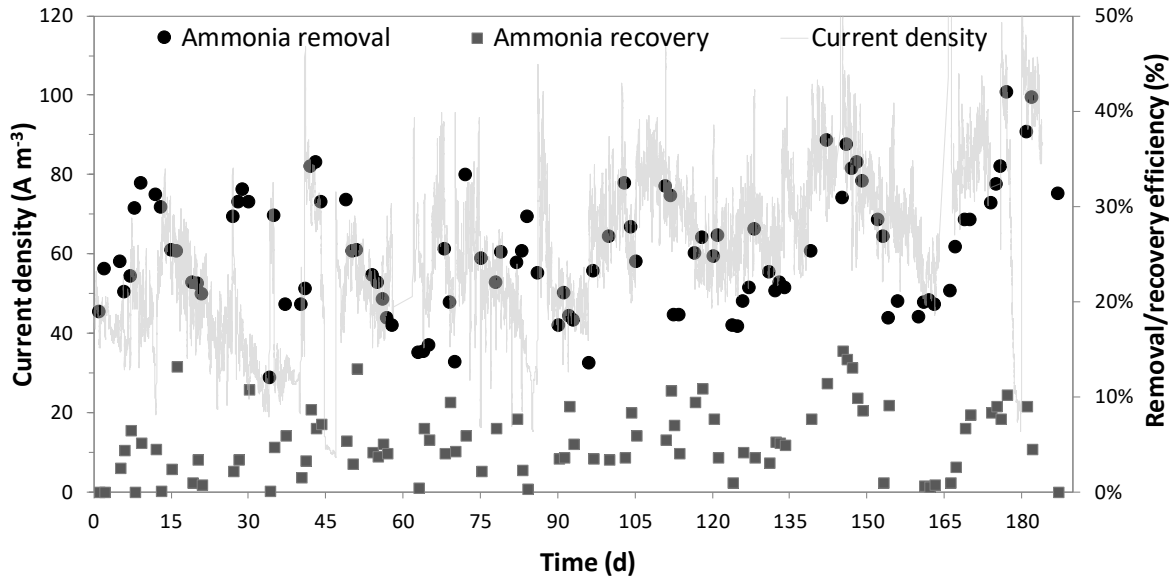
322 **Figure 3.** Ammonium removal and recovery efficiency in the catholyte and acid compartment in the HMS, with an initial  
 323  $\text{NH}_4^+\text{-N}$  concentration of  $500 \text{ mg L}^{-1}$  at a) pH 10, b) pH 11 and c) pH 12; and d) with an initial  $\text{NH}_4^+\text{-N}$  concentration of  $125$   
 324  $\text{mg L}^{-1}$  and pH 11.

325

### 326 **3.2. Performance and removal efficiencies of the MEC-S with synthetic feeding**

327 The HMS was connected in the recirculation circuit of the catholyte of the MEC-S  
328 after the characterisation of the ammonia flux through the hydrophobic membrane (section  
329 3.1). The MEC-S produced an average current density of  $47 \pm 25 \text{ A m}^{-3}$  (Figure 4), with a COD  
330 and an ammonium removal efficiency in the anode compartment of  $85 \pm 4\%$  and  $25 \pm 6\%$ ,  
331 respectively. Maximums of 40% ammonium removal efficiency were achieved in the periods  
332 with the highest current density (over  $100 \text{ A m}^{-3}$ ). The improvement in the current density  
333 during the last 20 days of operation allowed for an average ammonium recovery efficiency of  
334  $33 \pm 5\%$ , representing an average flux of  $0.3 \text{ g N m}^{-2} \text{ h}^{-1}$ . Ammonium removal efficiency is  
335 closely related to the behaviour of the current density, as previously reported [21]. The  
336 cathode effluent contained  $25 \pm 6\%$  of the ammonia fed to the anode compartment. The amount  
337 of ammonia recovered in the acid compartment of the HMS was fluctuating, with an average  
338 of  $7 \pm 3\%$ , which represents a recovery of  $29 \pm 17\%$  of the N transferred from the anode to the  
339 cathode compartment. Previous reports have shown an unstable transport across the  
340 hydrophobic membrane. Zamora et co-workers (2017) operated a urine-fed scaled-up MEC  
341 for ammonia recovery, achieving  $31 \pm 11\%$  nitrogen removal from the anode chamber [54].  
342 The cathode was connected to a trans-membrane chemisorption (TMCS) module for ammonia  
343 recovery. In that case, the average pH measured in the cathode was  $9.0 \pm 1.2$  so, due to this  
344 high fluctuation in the catholyte pH,  $\text{NH}_3$  was not always the dominant species and the  
345 transport over the TMCS was unstable ( $31 \pm 59\%$ ). The removal and recovery values obtained  
346 in that study are very similar to the results achieved in the synthetic operated MEC-S. Other  
347 studies have reported similar ammonium removal efficiencies, but achieving higher recovery  
348 efficiencies, such as Kuntke and co-workers (2016), who achieved an average ammonium-  
349 nitrogen removal of  $42 \pm 6\%$  in a continuous urine feed MEC, recovering in a punctual period  
350 of 5 days about 95% of the N removed from the anolyte in sulphuric acid [52]. In that study,

351 catholyte pH was  $9.5 \pm 0.2$ , so the higher pH stability, added to the fact that the cathode  
 352 compartment was operated in batch mode -achieving higher catholyte ammonia nitrogen  
 353 concentration, over  $800 \text{ mg L}^{-1}$ -, may have enhanced ammonia absorption in the acid solution.



354  
 355 **Figure 4.** Current density obtained with the operation of the MES-S in synthetic operation, ammonia removal efficiency  
 356 from the anode compartment and recovery efficiency in the acid compartment of the HMS.

357  
 358 As shown in Figure 4, ammonia recovery efficiency was higher in the periods with  
 359 higher current density, since more ammonia is transferred to the cathode compartment and a  
 360 higher pH value is achieved [22]. In these conditions, up to 48% of the ammonia transferred  
 361 to the cathode compartment was recovered, with a maximum flux of  $2.9 \text{ g N m}^{-2} \text{ h}^{-1}$ , slightly  
 362 lower to the result obtained in batch with the lower ammonium concentration ( $3.4 \pm 0.7 \text{ g N m}^{-2} \text{ h}^{-1}$   
 363  $^2 \text{ h}^{-1}$  with the initial concentration of  $125 \text{ mg L}^{-1}$  with a pH of 11). Furthermore, the increase  
 364 of the HRT of the catholyte compartment also increased the N flux through the hydrophobic  
 365 membrane, since pH and ammonium concentration of the catholyte increased. The average  
 366 flux through the hydrophobic membrane for the first 105 days of operation was of  $1.1 \pm 0.7 \text{ g}$   
 367  $\text{N m}^{-2} \text{ h}^{-1}$ , showing a high fluctuation, concomitant to a pH value of the cathodic bulk solution



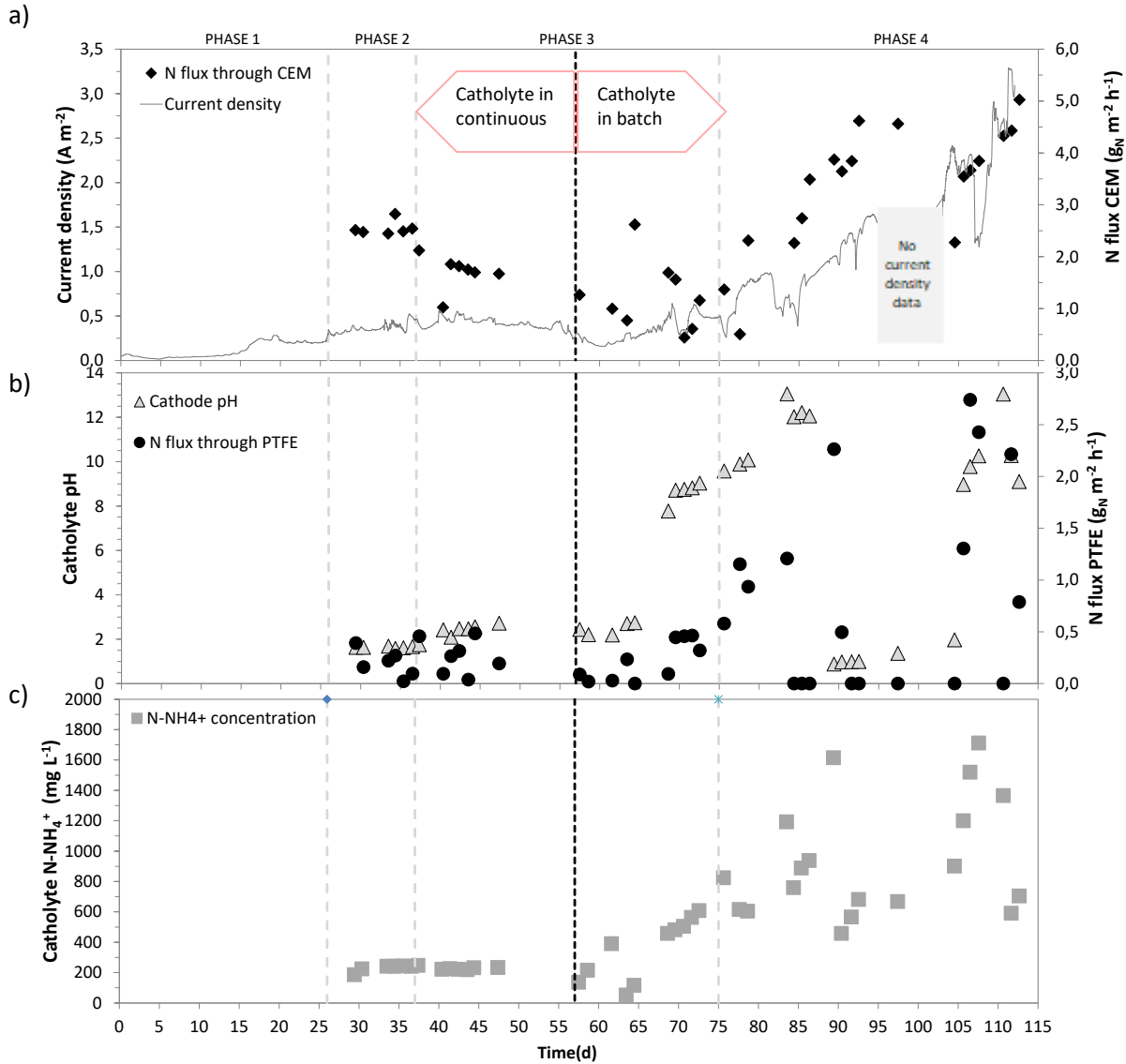
368 of  $11\pm 1$  and a N concentration of  $112\pm 33$  mg L<sup>-1</sup>. When the HRT was increased, the average  
369 flux increased 27% ( $1.4 \pm 0.9$  g N m<sup>-2</sup> h<sup>-1</sup>, pH of  $10\pm 1$  and N concentration of  $270\pm 98$  mg L<sup>-1</sup>).  
370

### 371 **3.3. Operation of the MECs with digestate feeding**

#### 372 3.3.1 Performance and COD removal efficiency

373 The operation with digested pig slurry of both MECs was started after inoculation and  
374 operation for a short period with synthetic media (data not shown) and the OLR and NLR was  
375 stepwise increased (Table 1). The current density obtained in MEC-H reactor gradually  
376 increased with the increase in OLR in each phase, especially in phase 4 (Figure 5a). The  
377 reference electrode had a malfunction between the day 96 and 104 during which no real data  
378 of the voltages and current intensity was provided by the potentiostat. After replacement of  
379 the reference electrode, the system quickly recovered its performance in terms of current  
380 density. Regarding the MEC-S, Figure 6a shows a more unstable performance in current  
381 density production than MEC-H, and in phase 4 the potential applied by the potentiostat was  
382 not constant because of overpotential in the system. In average, current density in the first 3  
383 phases were similar in both reactors, as shown in Table 2, while the performance in phase 4  
384 improved especially in the MEC-H, which achieved an average of  $1.40\pm 0.71$  A m<sup>-2</sup>, compared  
385 to  $0.61\pm 0.28$  A m<sup>-2</sup> in the MEC-S. Previous work of a MEC in sandwich configuration  
386 operated with digested pig slurry and a similar OLR achieved similar values for current  
387 density,  $1.59 \pm 0.70$  A m<sup>-2</sup> [21]. The average COD removal efficiency achieved  $21\pm 7\%$  and  
388  $16\pm 6\%$  in the MEC-H and the MEC-S, respectively. The decrease in COD removal efficiency  
389 with respect to the synthetic operation with acetate in the MEC-S (which achieved a COD  
390 removal efficiency of 85%) is consistent with previous studies with pig slurry digestate or  
391 food and agricultural wastes used as complex substrates [21,71], since simple substrates such  
392 as acetate are easier to degrade [72].

394



395

396

397

398

399

400

401

402

403

404

405

406

407

408

409

410

411

412

413

414

415

416

417

418

419

420

421

422

423

424

425

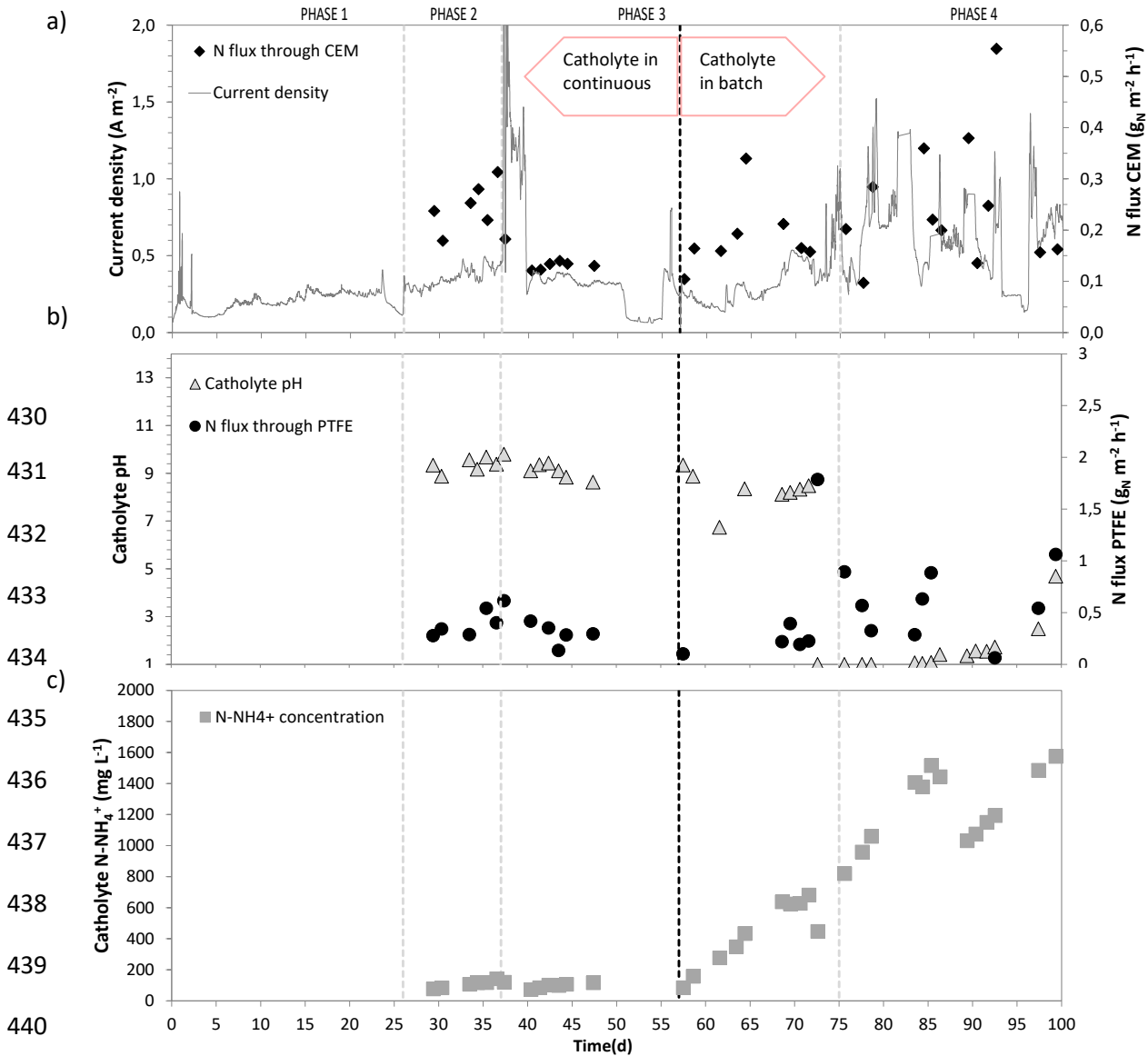
426

427

428

**Figure 5.** Current density obtained with the operation of the MES-H in digestate operation and nitrogen flux through the cationic exchange membrane (CEM) (a); nitrogen flux through the hydrophobic membrane (PTFE) and pH of the cathode compartment bulk solution (b); and nitrogen ammonium concentration in the cathode compartment bulk solution (c). The reference electrode had a malfunction on day 96 and was replaced on day 104, so data in this period was omitted in the figure.

429



441 **Figure 6.** Current density obtained with the operation of the MES-S in digestate operation and nitrogen flux through the  
 442 cationic exchange membrane (CEM) (a); nitrogen flux through the hydrophobic membrane (PTFE) and pH of the cathode  
 443 compartment bulk solution (b); and nitrogen ammonium concentration in the cathode compartment bulk solution (c).

444

### 445 3.3.2 Ammonium removal efficiency

446 Ammonium removal efficiency in the MEC-H achieved 23±1%, 17±3% and 18±5%  
 447 in phases 2, 3 and 4, respectively, compared to slightly lower values in the MEC-S (20±8%,  
 448 13±2% and 7±3% in phases 2, 3 and 4, respectively). The NH<sub>4</sub><sup>+</sup>-N flux by migration from the  
 449 anode to the cathode compartment in the MEC-H (Figure 5a) was in general an order of

450 magnitude higher than in the MEC-S (Figure 6a), achieving  $3.4 \pm 1.2 \text{ g N m}^{-2} \text{ h}^{-1}$  in phase 4  
451 (Table 2). These results can be explained by the different CEM surface in each reactor. As  
452 stated in the Materials and Methods section, the surface of the MEC-H CEM represented 12%  
453 of the MEC-S CEM, because of the system configuration. Therefore, with a similar current  
454 density, a similar amount of N was transferred through the CEM of both reactors, despite the  
455 smaller surface in the MEC-H CEM.

456 Ammonium removal in MEC is dependent on the current density, as described before  
457 [12]. In this study, a chronoamperometric operation mode was chosen, which involves poisoning  
458 the anode to a certain potential. If desired, to avoid oscillations in current density and N flux,  
459 a chronopotentiometric method could be also applied, fixing the current density in the external  
460 circuit. In this second option, anode potential may be less favourable for exoelectrogenic  
461 bacteria, since will change to a value dependent on several factors, including the substrate  
462 type and concentration, the applied voltage, and the specific microorganisms present [73].  
463 This could lead to lower COD removal efficiencies.

464 For a fixed current, various cations (generally  $\text{Na}^+$ ,  $\text{K}^+$ ,  $\text{Mg}^{2+}$ ,  $\text{Ca}^{2+}$ ) in the anolyte can  
465 compete with the  $\text{NH}_4^+$  ions for transport across the CEM, thus potentially compromising the  
466 removal of  $\text{NH}_4^+$  ions from the anolyte [74]. This phenomena has been extensively studied  
467 previously with raw and digested pig slurry, showing that  $\text{NH}_4^+$  acts as a primary charge  
468 carrier, accounting for 53%-67% of the migrated positive charges [75,76].

469 The flux through the CEM obtained in the MEC-S is half the  $0.54 \text{ g N m}^{-2} \text{ h}^{-1}$  obtained  
470 in previous studies with the same feeding substrate and configuration [21]. Differently, the  
471 high flux in the MEC-H is very similar to the one obtained with a submersible microbial  
472 desalination cell fed with synthetic solution [77].

473

474 **Table 2.** Main operational results (average  $\pm$  standard deviation) of the MECs during digestate feeding (CEM: cationic  
 475 exchange membrane; HM: hydrophobic membrane).

Phase		Current density (A m <sup>-2</sup> )	NH <sub>4</sub> <sup>+</sup> -N transference through the CEM (g m <sup>-2</sup> h <sup>-1</sup> )	NH <sub>4</sub> <sup>+</sup> -N transference through the HM (g m <sup>-2</sup> h <sup>-1</sup> )	NH <sub>4</sub> <sup>+</sup> -N concentration in the cathode compartment (mg L <sup>-1</sup> )	pH cathode compartment
MEC-S						
1		0.20 $\pm$ 0.07	-	-	-	-
2		0.36 $\pm$ 0.07	0.25 $\pm$ 0.05	0.4 $\pm$ 0.1	107 $\pm$ 24	9.3 $\pm$ 0.3
3	Cathode in continuous	0.37 $\pm$ 0.35	0.16 $\pm$ 0.06	0.3 $\pm$ 0.2	105 $\pm$ 26	9.2 $\pm$ 0.4
	Cathode in batch			0.6 $\pm$ 0.7		
4		0.61 $\pm$ 0.28	0.25 $\pm$ 0.13	0.7 $\pm$ 0.3	1238 $\pm$ 243	1.8 $\pm$ 1.1
MEC-H						
1		0.16 $\pm$ 0.08	-	-	-	-
2		0.35 $\pm$ 0.06	2.6 $\pm$ 0.1	0.2 $\pm$ 0.1	230 $\pm$ 23	1.6 $\pm$ 0.1
3	Cathode in continuous	0.38 $\pm$ 0.11	1.4 $\pm$ 0.6	0.3 $\pm$ 0.2	218 $\pm$ 34	2.4 $\pm$ 0.3
	Cathode in batch			0.3 $\pm$ 0.2		
4		1.40 $\pm$ 0.71	3.4 $\pm$ 1.2	1.5 $\pm$ 0.8	937 $\pm$ 384	10.8 $\pm$ 1.5

476

477 Although other ammonia removal technologies, such as stripping and absorption  
 478 [78,79], membrane distillation [80,81] or ionic exchange [82,83] have reported higher  
 479 removal efficiencies (>90%) than the obtained in this study, MEC present several advantages  
 480 over them. MEC operation generates the favourable pH for ammonia volatilisation with no  
 481 chemical addition nor temperature increase, differently from stripping and absorption process.  
 482 If digested pig slurry was operated directly with membrane distillation, also an increase of  
 483 pH, either by chemical addition or aeration, or temperature increase, would be needed to  
 484 improve removal efficiency. Regarding ion exchange, a previous step of solids and organic  
 485 matter removal would be needed to avoid clogging of the columns, and it is a process that has  
 486 to be operated by repeating adsorption and regeneration cycles in order to remove and recover  
 487 ammonia. Furthermore, ion exchange is more efficient at relative low pH (value of 6) [84],  
 488 while digested pig slurry used in this study had a pH value of 8.

### 489 3.3.3 Ammonium recovery efficiency

490  $\text{NH}_4^+$ -N flux through the hydrophobic membrane towards the recovery acid  
491 compartment presented a high variability in all the phases in both reactors, as shown in Figure  
492 5b (MEC-H) and Figure 6b (MEC-S).  $\text{NH}_4^+$ -N average transference increased from 0.2 and  
493  $0.4 \text{ g N m}^{-2} \text{ h}^{-1}$  in phase 2 in MEC-H and MEC-S, respectively, to 1.5 and  $0.7 \text{ g N m}^{-2} \text{ h}^{-1}$  in  
494 phase 4 (Table 2). Two factors had influence in these results: ammonia concentration in the  
495 cathode compartment and the pH of the bulk solution, as seen in the batch and continuous  
496 synthetic assays in this paper, and the results reported by other authors [34,69,70]. The pH  
497 value in the MEC-H cathode compartment was very low until half of phase 3 (Figure 5b),  
498 when the cathode compartment was operated in continuous mode. From day 57 on, the  
499 operation was switched to batch, in order to maintain a higher ammonia concentration in the  
500 cathode compartment (Figure 5c) and improve the N transference. This change also allowed  
501 for the increase in pH value, making it more favourable to the increase in the proportion of  
502 ammonia species. This way,  $\text{NH}_4^+$ -N in the cathode compartment increased from  $230 \pm 23 \text{ mg}$   
503  $\text{L}^{-1}$  in phase 2 to  $937 \pm 384 \text{ mg L}^{-1}$  in phase 4 (Table 2). In the case of the MEC-S, pH value in  
504 phase 2 and 3 was over 8 (Figure 6b), and although  $\text{NH}_4^+$ -N in the cathode compartment was  
505 half the value obtained in MEC-H in phase 2 and 3 (Figure 5c and Figure 6c), the  $\text{NH}_4^+$ -N  
506 flux through the hydrophobic membrane was similar or slightly higher. The switch from  
507 continuous operation to batch mode also allow for an increase in the  $\text{NH}_4^+$ -N cathode  
508 concentration, from  $107 \pm 24 \text{ mg L}^{-1}$  in phase 2 to  $1238 \pm 243 \text{ mg L}^{-1}$  in phase 4 (Table 2). This  
509 higher concentration may have improved the flux, due to the increase of the mass transfer  
510 driving force. Both reactors had a sharp decrease in the pH value in phase 4 after a change of  
511 the acidic solution in the recovery compartment, which drastically decreased the ammonia  
512 transference through the hydrophobic membrane until the pH increased to basic values. This  
513 behaviour was also observed during the synthetic MEC-S operation, but in that case the pH

514 decrease was overcome in one or two days after the acid change and the recovery efficiency  
515 recovered. The low pH of the new acid may promote, in the first hours after acid replacement,  
516 a high diffusion of the catholyte ammonia through the hydrophobic membrane, and a pH  
517 decrease. Although ammonium accumulated stepwise in the cathode compartment when  
518 batch operation started, the concentration decreased following acid replacement (Figure 5c  
519 and 6c). This adverse effect could be reduced with the circulation of the acid in a bigger tank,  
520 in order to minimise the frequency of the acid substitution, or by the substitution of part of  
521 the acid instead of the full recovery compartment.

522           Maximum flux through the hydrophobic membrane in the MEC-H was  $66 \text{ g N m}^{-2}$   
523  $\text{day}^{-1}$ , concomitant to a pH value of the cathode bulk solution of 9.8 and an  $\text{NH}_4^+\text{-N}$  cathode  
524 concentration of  $1520 \text{ mg L}^{-1}$ . This value is comparable to the one obtained in the MEC-S  
525 with synthetic feeding. The N flux through the hydrophobic membrane achieved by other  
526 authors, applied to anaerobic digestion technology, is very variable. It is in a range from  $1.48$   
527  $\text{g N m}^{-2} \text{ day}^{-1}$ , using a membrane contactor to recover ammonia from anaerobically digested  
528 chicken manure, operated with in sweep gas mode instead of using an acidic solution in  
529 contact with the membrane [70]; to  $89 \text{ g N m}^{-2} \text{ day}^{-1}$ , submerging a gas-permeable membrane  
530 (expanded PTFE) in a vessel filled with swine manure [33]. Table 3 shows a compilation of  
531 N flux reported in previous studies, working with different substrates and reactors.

532           Comparing both experimental configurations operated in this study, the 3 chamber  
533 MEC (MEC-H) has achieved better results regarding current density and N flux through the  
534 hydrophobic membrane than the MEC-S. Furthermore, the 3 chamber cell configuration is  
535 less complex than other experimental setups using gas recirculation [21,85,86] or a multiple  
536 absorption vessel [22]. It neither needs producing any overpressure to achieve the diffusion  
537 over a membrane contactor [52]. Hence, it reveals as an interesting configuration for further  
538 investigation and operation improvement. For example, continuous pH control and

539 automatised acid replacement would be necessari in the ARC to achieve a more stable  
 540 ammonia flux through the hydrophobic membrane.

541

542 **Table 3.** Compilation of N flux through hydrophobic membranes reported by previous studies. (MEC: Microbial electrolysis  
 543 cell; EC: Electrochemical cell; PTFE: polytetrafluoroethylene; ePTFE: expanded polytetrafluoroethylene; PP:  
 544 polypropylene; PDMS: polydimethylsiloxane.)

Substrate	Reactor/tank	Kind of membrane	Nitrogen flux (g m <sup>-2</sup> day <sup>-1</sup> )	Reference
Anaerobically digested pig slurry	MEC	Flat PTFE	66	This study
Anaerobically digested pig slurry	Tank	Tubular ePTFE	28	[36]
Anaerobically digested pig slurry	Tank	Tubular ePTFE	6	[28]
Anaerobically digested pig slurry	Tank	Tubular ePTFE	6	[28]
Anaerobically codigested pig slurry	Tank	Tubular ePTFE	60	[87]
Anaerobically digested pig slurry	Tank	Tubular ePTFE	6.6	[32]
Anaerobically digested dairy manure	Tank	Tubular ePTFE	51	[69]
Anaerobically digested chicken manure	Tank	Tubular PDMS	1.48	[70]
Poultry litter	Tank	Flat ePTFE	17.78	[35]
Swine manure	Tank	Tubular ePTFE	89	[33]
Swine manure	Tank	Tubular ePTFE	2.27	[34]
Swine manure	Tank	Tubular ePTFE	38	[38]
Swine manure	Tank	Tubular ePTFE	27.1	[37]
Urine	EC	Flat PTFE	94	[53]
Synthetic wastewater	EC	Flat PTFE	69	[61]
Centrate of anaerobically digested sewage sludge	Tank	Tubular ePTFE	133	[88]
Urine	EC	Flat PP	1010	[60]

545

546



### 547 **3.4. Electrochemical characterisation of the anode biofilm development**

548 The development of the anode biofilm of both MECs operated with digested pig slurry  
549 was evaluated through two monitoring tools, EIS tests and CV. Figure 7 shows the anode EIS  
550 spectra (Nyquist plots) observed in different days of operation both for the MEC-H and the  
551 MEC-S (see Supporting Information SI1 for a description of the curves observed and Figure  
552 SI1 and Figure SI2 for Bode plots).

553 Using the equivalent circuit shown in Figure 2, the  $R_{ct}$  of the anodes at different stages  
554 of the microbial growth was evaluated from the EIS data obtained on different days. On day  
555 20, were estimated to be  $30.8 \Omega$  and  $16.8 \Omega$  in the MEC-H and the MEC-S, respectively. This  
556 value decreased 89% during MEC-H operation, while only 16% in the MEC-S (Figure 8).  
557 This indicates that the microbial growth on the anode has a beneficial effect on the kinetics  
558 of the bio-electrochemical reaction as it decreases the anode activation losses due to increased  
559 biocatalyst density [89]. The reduction of the  $R_{ct}$  of the MEC-H anode is inversely  
560 proportional to the current density produced by the cell ( $R^2=0.9204$ ). This correlation was not  
561 observed in the MEC-S, although periods with higher  $R_{ct}$  corresponded in general with less  
562 current density production. The slight increase in  $R_{ct}$  during MEC-S operation, observed also  
563 in other studies [89] may be due to an increase in inactive biofilm for electrochemical  
564 reactions.

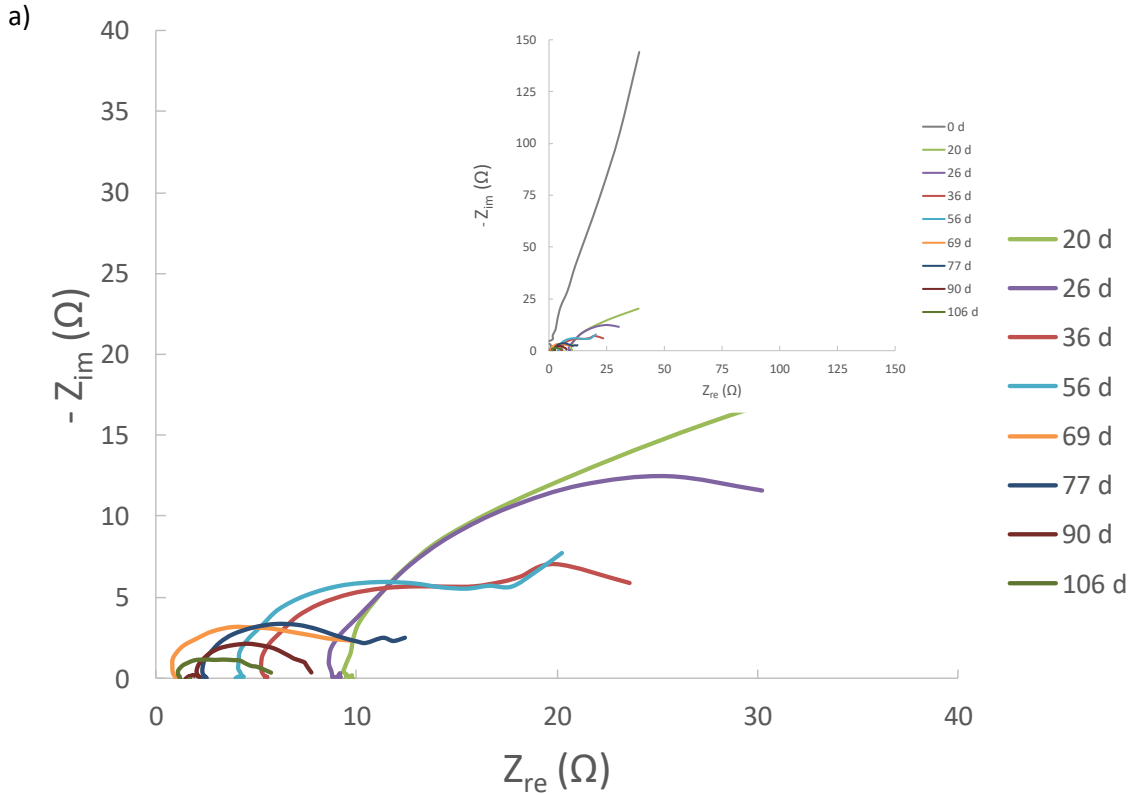
565 The evolution of the anode CV overtime was also assessed (Figure SI3) to compare  
566 with the information provided by the EIS tests. The MEC-H showed a clear increase in the  
567 current generated by the oxidation reaction with time, while the MEC-S showed lower current  
568 production than the MEC-H and a poorer improvement over time. The evolution of the CV in  
569 both reactors pointed to the proliferation of the anode-reducing microorganisms, consistent  
570 with the data obtained with the EIS test, and showing the different behaviour of both reactors.

571            In summary, the electrochemical methods used in this study showed that an increase  
572 in current density coincided with a progressive decrease of the anode internal resistance, as  
573 described before [64].

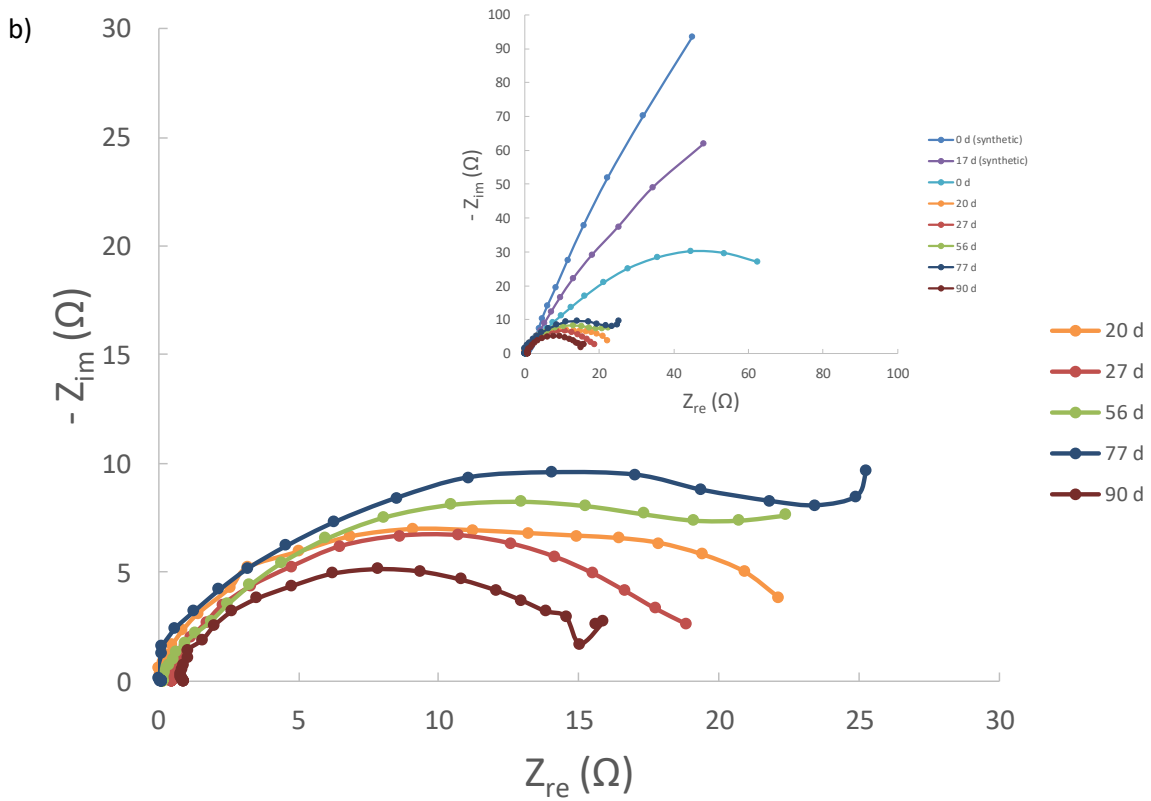
574

575

576

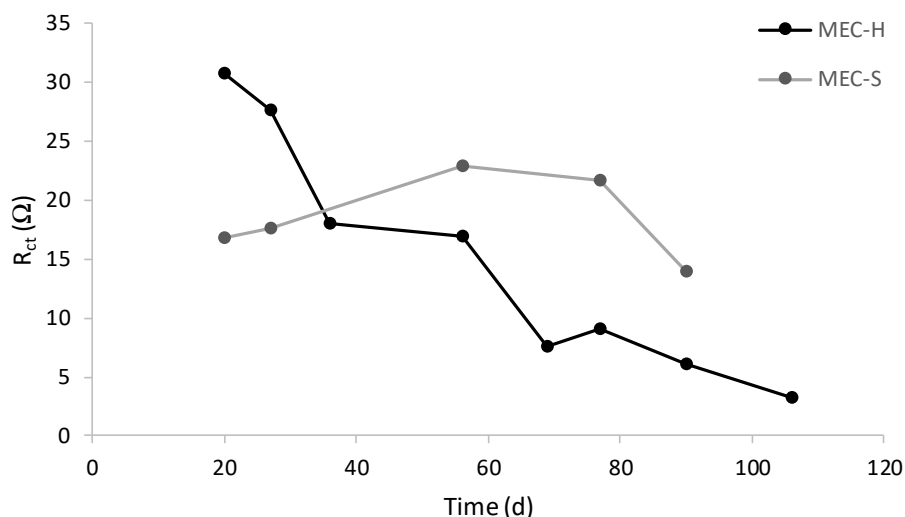


577



578

579 **Figure 7.** Anode electrochemical impedance spectroscopy spectra observed during 20-106 days of MEC-H operation, and  
 580 including day 0 in the inset (a). And during 20-90 days of MEC-S operation, including day 0 and day 17 in synthetic  
 581 operation and day 0 with digestate feeding in the inset (b).



582

583 **Figure 8.** Evolution of the  $R_{ct}$  in the MEC-H AND MEC-S.

584

#### 585 **4. Conclusions**

586 The combination of MECs with hydrophobic membranes reveals as a suitable  
 587 technology for the recovery of ammonia and treatment of high strength wastewater such as  
 588 livestock manure, either in a configuration with the membrane in contact with the cathode  
 589 compartment or in the catholyte recirculation circuit. Ammonia removal from the substrate  
 590 was directly linked to the current density produced by the cell, which in turn was correlated  
 591 to the development of biofilm in the anode. This biofilm evolution has been monitored by  
 592 electrochemical techniques (CV and EIS test) and its relationship with the anode resistance  
 593 has been assessed. In turn, the diffusion of ammonia through the gas permeable membranes  
 594 was enhanced with the catholyte ammonium content and pH, achieving a maximum flux of  
 595  $66 \text{ g N m}^{-2} \text{ day}^{-1}$ . The evolution of the cathode pH during MEC operation avoids the addition  
 596 of alkali or aeration, compared to the direct use of hydrophobic membranes in anaerobic  
 597 digestion. Compared to a stripping and absorption system coupled to MECs, the use of  
 598 hydrophobic membranes for N recovery avoids electricity consumption for air pumping.  
 599 Furthermore, the 3-chamber cell configuration (MEC-H) simplifies the operation of the

600 recovery of ammonia, but improvement is still needed to stabilise the flux of ammonia  
601 through the hydrophobic membrane, highly dependent on catholyte and recovery acid pH.

602

### 603 **Declaration of competing interest**

604 The authors declare that they have no known competing financial interests or personal  
605 relationships that could have appeared to influence the work reported in this paper.

606

### 607 **Acknowledgements**

608 This research was funded by the Spanish Ministry of Economy and Competitiveness  
609 (INIA project RTA2015-00079-C02-01). The support of the CERCA Program and of the  
610 Consolidated Research Group TERRA (ref. 2017 SGR 1290), both from the Generalitat de  
611 Catalunya, is also acknowledged.

612

### 613 **References**

614

- 615 [1] Q. Schiermeier, J. Tollefson, T. Scully, A. Witze, O. Morton, Energy alternatives:  
616 Electricity without carbon, *Nature*. 454 (2008) 816–823.  
617 <https://doi.org/10.1038/454816a>.
- 618 [2] L. Alibardi, T.F. Astrup, F. Asunis, W.P. Clarke, G. De Gioannis, P. Dessì, P.N.L.  
619 Lens, M.C. Lavagnolo, L. Lombardi, A. Muntoni, A. Pivato, A. Poletini, R. Pomi, A.  
620 Rossi, A. Spagni, D. Spiga, Organic waste biorefineries: Looking towards  
621 implementation, *Waste Manag.* 114 (2020) 274–286.  
622 <https://doi.org/https://doi.org/10.1016/j.wasman.2020.07.010>.
- 623 [3] G. Moretto, I. Russo, D. Bolzonella, P. Pavan, M. Majone, F. Valentino, An urban  
624 biorefinery for food waste and biological sludge conversion into  
625 polyhydroxyalkanoates and biogas, *Water Res.* 170 (2020) 115371.  
626 <https://doi.org/https://doi.org/10.1016/j.watres.2019.115371>.
- 627 [4] D. Pant, A. Singh, G. Van Bogaert, S. Irving Olsen, P. Singh Nigam, L. Diels, K.  
628 Vanbroekhoven, Bioelectrochemical systems (BES) for sustainable energy production  
629 and product recovery from organic wastes and industrial wastewaters, *RSC Adv.* 2  
630 (2012) 1248–1263. <https://doi.org/10.1039/c1ra00839k>.
- 631 [5] S.G. Barbosa, T. Rodrigues, L. Peixoto, P. Kuntke, M.M. Alves, M.A. Pereira, A. Ter  
632 Heijne, Anaerobic biological fermentation of urine as a strategy to enhance the  
633 performance of a microbial electrolysis cell (MEC), *Renew. Energy.* 139 (2019) 936–  
634 943. <https://doi.org/https://doi.org/10.1016/j.renene.2019.02.120>.
- 635 [6] M. Cerrillo, M. Viñas, A. Bonmatí, Anaerobic digestion and electromethanogenic  
636 microbial electrolysis cell integrated system: Increased stability and recovery of  
637 ammonia and methane, *Renew. Energy.* 120 (2018) 178–189.

- 638 <https://doi.org/https://doi.org/10.1016/j.renene.2017.12.062>.
- 639 [7] A. Hassanein, F. Witarasa, X. Guo, L. Yong, S. Lansing, L. Qiu, Next generation  
640 digestion: Complementing anaerobic digestion (AD) with a novel microbial  
641 electrolysis cell (MEC) design, *Int. J. Hydrogen Energy*. 42 (2017) 28681–28689.  
642 <https://doi.org/https://doi.org/10.1016/j.ijhydene.2017.10.003>.
- 643 [8] M. Cerrillo, M. Viñas, A. Bonmatí, Unravelling the active microbial community in a  
644 thermophilic anaerobic digester-microbial electrolysis cell coupled system under  
645 different conditions, *Water Res.* 110 (2017) 192–201.  
646 <https://doi.org/https://doi.org/10.1016/j.watres.2016.12.019>.
- 647 [9] P. Kuntke, T.H.J.A. Sleutels, M. Rodríguez Arredondo, S. Georg, S.G. Barbosa, A. ter  
648 Heijne, H.V.M. Hamelers, C.J.N. Buisman, (Bio)electrochemical ammonia recovery:  
649 progress and perspectives, *Appl. Microbiol. Biotechnol.* 102 (2018) 3865–3878.  
650 <https://doi.org/10.1007/s00253-018-8888-6>.
- 651 [10] A. Sotres, M. Cerrillo, M. Viñas, A. Bonmatí, Nitrogen recovery from pig slurry in a  
652 two-chambered bioelectrochemical system, *Bioresour. Technol.* 194 (2015) 373–382.  
653 <https://doi.org/https://doi.org/10.1016/j.biortech.2015.07.036>.
- 654 [11] M.B. Vanotti, A.A. Szogi, P.D. Millner, J.H. Loughrin, Development of a second-  
655 generation environmentally superior technology for treatment of swine manure in the  
656 USA, *Bioresour. Technol.* 100 (2009) 5406–5416.  
657 <https://doi.org/https://doi.org/10.1016/j.biortech.2009.02.019>.
- 658 [12] M. Cerrillo, M. Viñas, A. Bonmatí, Microbial fuel cells for polishing effluents of  
659 anaerobic digesters under inhibition, due to organic and nitrogen overloads, *J. Chem.*  
660 *Technol. Biotechnol.* 92 (2017) 2912–2920. <https://doi.org/10.1002/jctb.5308>.
- 661 [13] M. Rodríguez Arredondo, P. Kuntke, A. ter Heijne, H.V.M. Hamelers, C.J.N. Buisman,  
662 Load ratio determines the ammonia recovery and energy input of an electrochemical  
663 system, *Water Res.* 111 (2017) 330–337.  
664 <https://doi.org/https://doi.org/10.1016/j.watres.2016.12.051>.
- 665 [14] J. De Paepe, K. De Paepe, F. Gòdia, K. Rabaey, S.E. Vlaeminck, P. Clauwaert, Bio-  
666 electrochemical COD removal for energy-efficient, maximum and robust nitrogen  
667 recovery from urine through membrane aerated nitrification, *Water Res.* 185 (2020)  
668 116223. <https://doi.org/https://doi.org/10.1016/j.watres.2020.116223>.
- 669 [15] B. Virdis, K. Rabaey, Z. Yuan, J. Keller, Microbial fuel cells for simultaneous carbon  
670 and nitrogen removal, *Water Res.* 42 (2008) 3013–3024.  
671 <https://doi.org/https://doi.org/10.1016/j.watres.2008.03.017>.
- 672 [16] M.I. San-Martín, R. Mateos, A. Escapa, A. Morán, Understanding nitrogen recovery  
673 from wastewater with a high nitrogen concentration using microbial electrolysis cells,  
674 *J. Environ. Sci. Heal. Part A.* 54 (2019) 472–477.  
675 <https://doi.org/10.1080/10934529.2019.1567185>.
- 676 [17] M. Rodríguez Arredondo, P. Kuntke, A.W. Jeremiasse, T.H.J.A. Sleutels, C.J.N.  
677 Buisman, A. ter Heijne, Bioelectrochemical systems for nitrogen removal and recovery  
678 from wastewater, *Environ. Sci. Water Res. Technol.* 1 (2015) 22–33.  
679 <https://doi.org/10.1039/C4EW00066H>.
- 680 [18] P. Ledezma, P. Kuntke, C.J.N. Buisman, J. Keller, S. Freguia, Source-separated urine  
681 opens golden opportunities for microbial electrochemical technologies, *Trends*  
682 *Biotechnol.* 33 (2015) 214–220.  
683 <https://doi.org/https://doi.org/10.1016/j.tibtech.2015.01.007>.
- 684 [19] A. Bonmatí, X. Flotats, Air stripping of ammonia from pig slurry: characterisation and  
685 feasibility as a pre- or post-treatment to mesophilic anaerobic digestion, *Waste Manag.*  
686 23 (2003) 261–272. [https://doi.org/https://doi.org/10.1016/S0956-053X\(02\)00144-7](https://doi.org/https://doi.org/10.1016/S0956-053X(02)00144-7).
- 687 [20] M. Laureni, J. Palatsi, M. Llovera, A. Bonmatí, Influence of pig slurry characteristics

- 688 on ammonia stripping efficiencies and quality of the recovered ammonium-sulfate  
689 solution, *J. Chem. Technol. Biotechnol.* 88 (2013) 1654–1662.  
690 <https://doi.org/10.1002/jctb.4016>.
- 691 [21] M. Cerrillo, M. Viñas, A. Bonmatí, Overcoming organic and nitrogen overload in  
692 thermophilic anaerobic digestion of pig slurry by coupling a microbial electrolysis cell,  
693 *Bioresour. Technol.* 216 (2016) 362–372.  
694 <https://doi.org/https://doi.org/10.1016/j.biortech.2016.05.085>.
- 695 [22] X. Wu, O. Modin, Ammonium recovery from reject water combined with hydrogen  
696 production in a bioelectrochemical reactor, *Bioresour. Technol.* 146 (2013) 530–536.  
697 <https://doi.org/https://doi.org/10.1016/j.biortech.2013.07.130>.
- 698 [23] E.E. Licon Bernal, A. Alcaraz, S. Casas, C. Valderrama, J.L. Cortina, Trace ammonium  
699 removal by liquid–liquid membrane contactors as water polishing step of water  
700 electrolysis for hydrogen production from a wastewater treatment plant effluent, *J.*  
701 *Chem. Technol. Biotechnol.* 91 (2016) 2983–2993.  
702 <https://doi.org/https://doi.org/10.1002/jctb.4923>.
- 703 [24] W. Rongwong, K. Goh, Resource recovery from industrial wastewaters by  
704 hydrophobic membrane contactors: A review, *J. Environ. Chem. Eng.* 8 (2020)  
705 104242. <https://doi.org/https://doi.org/10.1016/j.jece.2020.104242>.
- 706 [25] W. Rongwong, S. Sairiam, A modeling study on the effects of pH and partial wetting  
707 on the removal of ammonia nitrogen from wastewater by membrane contactors, *J.*  
708 *Environ. Chem. Eng.* 8 (2020) 104240.  
709 <https://doi.org/https://doi.org/10.1016/j.jece.2020.104240>.
- 710 [26] M. Darestani, V. Haigh, S.J. Couperthwaite, G.J. Millar, L.D. Nghiem, Hollow fibre  
711 membrane contactors for ammonia recovery: Current status and future developments,  
712 *J. Environ. Chem. Eng.* 5 (2017) 1349–1359.  
713 <https://doi.org/https://doi.org/10.1016/j.jece.2017.02.016>.
- 714 [27] A. Bayrakdar, R.Ö. Sürmeli, B. Çalli, Anaerobic digestion of chicken manure by a  
715 leach-bed process coupled with side-stream membrane ammonia separation,  
716 *Bioresour. Technol.* 258 (2018) 41–47.  
717 <https://doi.org/https://doi.org/10.1016/j.biortech.2018.02.117>.
- 718 [28] P.J. Dube, M.B. Vanotti, A.A. Szogi, M.C. García-González, Enhancing recovery of  
719 ammonia from swine manure anaerobic digester effluent using gas-permeable  
720 membrane technology, *Waste Manag.* 49 (2016) 372–377.  
721 <https://doi.org/https://doi.org/10.1016/j.wasman.2015.12.011>.
- 722 [29] B. Lauterböck, M. Nikolausz, Z. Lv, M. Baumgartner, G. Liebhard, W. Fuchs,  
723 Improvement of anaerobic digestion performance by continuous nitrogen removal with  
724 a membrane contactor treating a substrate rich in ammonia and sulfide, *Bioresour.*  
725 *Technol.* 158 (2014) 209–216.  
726 <https://doi.org/https://doi.org/10.1016/j.biortech.2014.02.012>.
- 727 [30] B. Molinuevo-Salces, B. Riaño, M.B. Vanotti, M.C. García-González, Gas-permeable  
728 membrane technology coupled with anaerobic digestion for swine manure treatment,  
729 *Front. Sustain. Food Syst.* 2 (2018). <https://doi.org/10.3389/fsufs.2018.00025>.
- 730 [31] G. Noriega-Hevia, J. Serralta, L. Borrás, A. Seco, J. Ferrer, Nitrogen recovery using a  
731 membrane contactor: Modelling nitrogen and pH evolution, *J. Environ. Chem. Eng.* 8  
732 (2020) 103880. <https://doi.org/https://doi.org/10.1016/j.jece.2020.103880>.
- 733 [32] I. González-García, B. Riaño, B. Molinuevo-Salces, M.B. Vanotti, M.C. García-  
734 González, Improved anaerobic digestion of swine manure by simultaneous ammonia  
735 recovery using gas-permeable membranes, *Water Res.* 190 (2021) 116789.  
736 <https://doi.org/https://doi.org/10.1016/j.watres.2020.116789>.
- 737 [33] S. Daguerre-Martini, M.B. Vanotti, M. Rodríguez-Pastor, A. Rosal, R. Moral, Nitrogen

- 738 recovery from wastewater using gas-permeable membranes: Impact of inorganic  
739 carbon content and natural organic matter, *Water Res.* 137 (2018) 201–210.  
740 <https://doi.org/https://doi.org/10.1016/j.watres.2018.03.013>.
- 741 [34] M.C. Garcia-González, M.B. Vanotti, Recovery of ammonia from swine manure using  
742 gas-permeable membranes: Effect of waste strength and pH, *Waste Manag.* 38 (2015)  
743 455–461. <https://doi.org/https://doi.org/10.1016/j.wasman.2015.01.021>.
- 744 [35] M.J. Rothrock, A.A. Szögi, M.B. Vanotti, Recovery of ammonia from poultry litter  
745 using flat gas permeable membranes, *Waste Manag.* 33 (2013) 1531–1538.  
746 <https://doi.org/https://doi.org/10.1016/j.wasman.2013.03.011>.
- 747 [36] M.B. Vanotti, P.J. Dube, A.A. Szögi, M.C. García-González, Recovery of ammonia  
748 and phosphate minerals from swine wastewater using gas-permeable membranes,  
749 *Water Res.* 112 (2017) 137–146.  
750 <https://doi.org/https://doi.org/10.1016/j.watres.2017.01.045>.
- 751 [37] B. Riaño, B. Molinuevo-Salces, M.B. Vanotti, M.C. García-González, Application of  
752 gas-permeable membranes for-semi-continuous ammonia recovery from swine  
753 manure, *Environ. - MDPI.* 6 (2019). <https://doi.org/10.3390/environments6030032>.
- 754 [38] B. Molinuevo-Salces, B. Riaño, M.B. Vanotti, D. Hernández-González, M.C. García-  
755 González, Pilot-scale demonstration of membrane-based nitrogen recovery from swine  
756 manure, *Membranes (Basel).* 10 (2020) 1–13.  
757 <https://doi.org/10.3390/membranes10100270>.
- 758 [39] M.A. Boehler, A. Heisele, A. Seyfried, M. Grömping, H. Siegrist, (NH<sub>4</sub>)<sub>2</sub>SO<sub>4</sub>  
759 recovery from liquid side streams, *Environ. Sci. Pollut. Res.* 22 (2015) 7295–7305.  
760 <https://doi.org/10.1007/s11356-014-3392-8>.
- 761 [40] B. Norddahl, V.G. Horn, M. Larsson, J.H. du Preez, K. Christensen, A membrane  
762 contactor for ammonia stripping, pilot scale experience and modeling, *Desalination.*  
763 199 (2006) 172–174. <https://doi.org/https://doi.org/10.1016/j.desal.2006.03.037>.
- 764 [41] B. Brennan, C. Briciu-Burghina, S. Hickey, T. Abadie, S.M. Al Ma Awali, Y. Delaure,  
765 J. Durkan, L. Holland, B. Quilty, M. Tajparast, C. Pulit, L. Fitzsimons, K. Nolan, F.  
766 Regan, J. Lawler, Pilot scale study: First demonstration of hydrophobic membranes for  
767 the removal of ammonia molecules from rendering condensate wastewater, *Int. J. Mol.*  
768 *Sci.* 21 (2020) 1–20. <https://doi.org/10.3390/ijms21113914>.
- 769 [42] M. Böhler, J. Fleiner, W. Gruber, A. Seyfried, L. Luning, D. Traksel, Powerstep: WP4:  
770 Nitrogen management in side stream D4.2: Planning and Design of a full- scale  
771 membrane ammonia stripping, 2016.
- 772 [43] L. Richter, M. Wichern, M. Grömping, U. Robecke, J. Haberkamp, Ammonium  
773 recovery from process water of digested sludge dewatering by membrane contactors,  
774 *Water Pract. Technol.* 15 (2020) 84–91. <https://doi.org/10.2166/wpt.2020.002>.
- 775 [44] M. Ulbricht, J. Schneider, M. Stasiak, A. Sengupta, Ammonia recovery from industrial  
776 wastewater by transMembranechemiSorption, *Chemie-Ingenieur-Technik.* 85 (2013)  
777 1259–1262. <https://doi.org/10.1002/cite.201200237>.
- 778 [45] W. Lee, S. An, Y. Choi, Ammonia harvesting via membrane gas extraction at  
779 moderately alkaline pH: A step toward net-profitable nitrogen recovery from domestic  
780 wastewater, *Chem. Eng. J.* 405 (2021) 126662.  
781 <https://doi.org/https://doi.org/10.1016/j.cej.2020.126662>.
- 782 [46] F. Nosratinia, M. Ghadiri, H. Ghahremani, Mathematical modeling and numerical  
783 simulation of ammonia removal from wastewaters using membrane contactors, *J. Ind.*  
784 *Eng. Chem.* 20 (2014) 2958–2963.  
785 <https://doi.org/https://doi.org/10.1016/j.jiec.2013.10.065>.
- 786 [47] E. Guillen-Burrieza, M.O. Mavukkandy, M.R. Bilad, H.A. Arafat, Understanding  
787 wetting phenomena in membrane distillation and how operational parameters can



- 788 affect it, *J. Memb. Sci.* 515 (2016) 163–174.  
 789 <https://doi.org/https://doi.org/10.1016/j.memsci.2016.05.051>.
- 790 [48] A. Zarebska, D.R. Nieto, K. V Christensen, B. Norddahl, Ammonia recovery from  
 791 agricultural wastes by membrane distillation: Fouling characterization and mechanism,  
 792 *Water Res.* 56 (2014) 1–10.  
 793 <https://doi.org/https://doi.org/10.1016/j.watres.2014.02.037>.
- 794 [49] L. He, Y. Wang, T. Zhou, Y. Zhao, Enhanced ammonia resource recovery from  
 795 wastewater using a novel flat sheet gas-permeable membrane, *Chem. Eng. J.* 400  
 796 (2020) 125338. <https://doi.org/https://doi.org/10.1016/j.cej.2020.125338>.
- 797 [50] H. Wang, X. Zhao, C. He, Constructing a novel zwitterionic surface of PVDF  
 798 membrane through the assembled chitosan and sodium alginate, *Int. J. Biol. Macromol.*  
 799 87 (2016) 443–448. <https://doi.org/https://doi.org/10.1016/j.ijbiomac.2016.02.074>.
- 800 [51] P.S. Goh, R. Naim, M. Rahbari-Sisakht, A.F. Ismail, Modification of membrane  
 801 hydrophobicity in membrane contactors for environmental remediation, *Sep. Purif.*  
 802 *Technol.* 227 (2019) 115721.  
 803 <https://doi.org/https://doi.org/10.1016/j.seppur.2019.115721>.
- 804 [52] P. Kuntke, P. Zamora, M. Saakes, C.J.N. Buisman, H.V.M. Hamelers, Gas-permeable  
 805 hydrophobic tubular membranes for ammonia recovery in bio-electrochemical  
 806 systems, *Environ. Sci. Water Res. Technol.* 2 (2016) 261–265.  
 807 <https://doi.org/10.1039/c5ew00299k>.
- 808 [53] M.E.R. Christiaens, K.M. Udert, J.B.A. Arends, S. Huysman, L. Vanhaecke, E.  
 809 McAdam, K. Rabaey, Membrane stripping enables effective electrochemical ammonia  
 810 recovery from urine while retaining microorganisms and micropollutants, *Water Res.*  
 811 150 (2019) 349–357. <https://doi.org/10.1016/j.watres.2018.11.072>.
- 812 [54] P. Zamora, T. Georgieva, A. Ter Heijne, T.H.J.A. Sleutels, A.W. Jeremiasse, M.  
 813 Saakes, C.J.N. Buisman, P. Kuntke, Ammonia recovery from urine in a scaled-up  
 814 Microbial Electrolysis Cell, *J. Power Sources.* 356 (2017) 491–499.  
 815 <https://doi.org/https://doi.org/10.1016/j.jpowsour.2017.02.089>.
- 816 [55] P. Kuntke, M. Rodrigues, T. Sleutels, M. Saakes, H.V.M. Hamelers, C.J.N. Buisman,  
 817 Energy-efficient ammonia recovery in an up-scaled hydrogen gas recycling  
 818 electrochemical system, *ACS Sustain. Chem. Eng.* 6 (2018) 7638–7644.  
 819 <https://doi.org/10.1021/acssuschemeng.8b00457>.
- 820 [56] T.H.J.A. Sleutels, B.J. Hoogland, P. Kuntke, A. ter Heijne, C.J.N. Buisman, H.V.M.  
 821 Hamelers, Gas-permeable hydrophobic membranes enable transport of CO<sub>2</sub> and NH<sub>3</sub>  
 822 to improve performance of bioelectrochemical systems, *Environ. Sci. Water Res.*  
 823 *Technol.* 2 (2016) 743–748. <https://doi.org/10.1039/C6EW00087H>.
- 824 [57] M. Rodrigues, T.T. De Mattos, T. Sleutels, A. Ter Heijne, H.V.M. Hamelers, C.J.N.  
 825 Buisman, P. Kuntke, Minimal bipolar membrane cell configuration for scaling up  
 826 ammonium recovery, *ACS Sustain. Chem. Eng.* 8 (2020) 17359–17367.  
 827 <https://doi.org/10.1021/acssuschemeng.0c05043>.
- 828 [58] M. Rodrigues, T. Sleutels, P. Kuntke, D. Hoekstra, A. ter Heijne, C.J.N. Buisman,  
 829 H.V.M. Hamelers, Exploiting Donnan Dialysis to enhance ammonia recovery in an  
 830 electrochemical system, *Chem. Eng. J.* 395 (2020) 125143.  
 831 <https://doi.org/https://doi.org/10.1016/j.cej.2020.125143>.
- 832 [59] P. Kuntke, M. Rodríguez Arredondo, L. Widyakristi, A. ter Heijne, T.H.J.A. Sleutels,  
 833 H.V.M. Hamelers, C.J.N. Buisman, Hydrogen gas recycling for energy efficient  
 834 ammonia recovery in electrochemical systems, *Environ. Sci. Technol.* 51 (2017) 3110–  
 835 3116. <https://doi.org/10.1021/acs.est.6b06097>.
- 836 [60] W.A. Tarpeh, J.M. Barazesh, T.Y. Cath, K.L. Nelson, Electrochemical Stripping to  
 837 Recover Nitrogen from Source-Separated Urine, *Environ. Sci. Technol.* 52 (2018)

- 1453–1460. <https://doi.org/10.1021/acs.est.7b05488>.
- [61] A. Iddya, D. Hou, C.M. Khor, Z. Ren, J. Tester, R. Posmanik, A. Gross, D. Jassby, Efficient ammonia recovery from wastewater using electrically conducting gas stripping membranes, *Environ. Sci. Nano.* 7 (2020) 1759–1771. <https://doi.org/10.1039/C9EN01303B>.
- [62] M.J. Liu, B.S. Neo, W.A. Tarpeh, Building an operational framework for selective nitrogen recovery via electrochemical stripping, *Water Res.* 169 (2020) 115226. <https://doi.org/https://doi.org/10.1016/j.watres.2019.115226>.
- [63] T. Sleutels, S. Molenaar, A. Heijne, C. Buisman, Low substrate loading limits methanogenesis and leads to high coulombic efficiency in bioelectrochemical systems, *Microorganisms.* 4 (2016) 7. <https://doi.org/10.3390/microorganisms4010007>.
- [64] E. Martin, O. Savadogo, S.R. Guiot, B. Tartakovsky, Electrochemical characterization of anodic biofilm development in a microbial fuel cell., *J. Appl. Electrochem.* 43 (2013) 533–540.
- [65] A. ter Heijne, O. Schaetzle, S. Gimenez, L. Navarro, B. Hamelers, F. Fabregat-Santiago, Analysis of bio-anode performance through electrochemical impedance spectroscopy, *Bioelectrochemistry.* 106 (2015) 64–72. <https://doi.org/https://doi.org/10.1016/j.bioelechem.2015.04.002>.
- [66] Standard Methods For the Examination of Water and Wastewater, American Public Health Association, 2018. <https://doi.org/doi:10.2105/SMWW.2882.036>.
- [67] V.F. Lvovich, Impedance Spectroscopy: Applications to Electrochemical and Dielectric Phenomena, 2012. <https://doi.org/10.1002/9781118164075>.
- [68] X. Dominguez-Benetton, S. Sevda, K. Vanbroekhoven, D. Pant, The accurate use of impedance analysis for the study of microbial electrochemical systems, *Chem. Soc. Rev.* 41 (2012) 7228–7246. <https://doi.org/10.1039/c2cs35026b>.
- [69] M. Fillingham, A.C. VanderZaag, J. Singh, S. Burt, A. Crolla, C. Kinsley, J.D. MacDonald, Characterizing the performance of gas-permeable membranes as an ammonia recovery strategy from anaerobically digested dairy manure, *Membranes (Basel).* 7 (2017) 1–13. <https://doi.org/10.3390/membranes7040059>.
- [70] R.Ö. Sürmeli, A. Bayrakdar, B. Çalli, Ammonia recovery from chicken manure digestate using polydimethylsiloxane membrane contactor, *J. Clean. Prod.* 191 (2018) 99–104. <https://doi.org/https://doi.org/10.1016/j.jclepro.2018.04.138>.
- [71] A. ElMekawy, S. Srikanth, S. Bajracharya, H.M. Hegab, P.S. Nigam, A. Singh, S.V. Mohan, D. Pant, Food and agricultural wastes as substrates for bioelectrochemical system (BES): The synchronized recovery of sustainable energy and waste treatment, *Food Res. Int.* 73 (2015) 213–225. <https://doi.org/https://doi.org/10.1016/j.foodres.2014.11.045>.
- [72] D. Pant, G. Van Bogaert, L. Diels, K. Vanbroekhoven, A review of the substrates used in microbial fuel cells (MFCs) for sustainable energy production, *Bioresour. Technol.* 101 (2010) 1533–1543. <https://doi.org/https://doi.org/10.1016/j.biortech.2009.10.017>.
- [73] J.-Y. Nam, J.C. Tokash, B.E. Logan, Comparison of microbial electrolysis cells operated with added voltage or by setting the anode potential, *Int. J. Hydrogen Energy.* 36 (2011) 10550–10556. <https://doi.org/https://doi.org/10.1016/j.ijhydene.2011.05.148>.
- [74] Y. Liu, M. Qin, S. Luo, Z. He, R. Qiao, Understanding ammonium transport in bioelectrochemical systems towards its recovery, *Sci. Rep.* 6 (2016) 22547. <https://doi.org/10.1038/srep22547>.
- [75] M. Cerrillo, J. Oliveras, M. Viñas, A. Bonmatí, Comparative assessment of raw and digested pig slurry treatment in bioelectrochemical systems, *Bioelectrochemistry.* 110 (2016) 69–78. <https://doi.org/https://doi.org/10.1016/j.bioelechem.2016.03.004>.

- 888 [76] G. Lee, K. Kim, J. Chung, J.-I. Han, Electrochemical ammonia accumulation and  
889 recovery from ammonia-rich livestock wastewater, *Chemosphere*. (2020) 128631.  
890 <https://doi.org/https://doi.org/10.1016/j.chemosphere.2020.128631>.
- 891 [77] Y. Zhang, I. Angelidaki, Counteracting ammonia inhibition during anaerobic digestion  
892 by recovery using submersible microbial desalination cell, *Biotechnol. Bioeng.* 112  
893 (2015) 1478–1482. <https://doi.org/10.1002/bit.25549>.
- 894 [78] L. Kinidi, I.A.W. Tan, N.B. Abdul Wahab, K.F. Bin Tamrin, C.N. Hipolito, S.F. Salleh,  
895 Recent development in ammonia stripping process for industrial wastewater treatment,  
896 *Int. J. Chem. Eng.* 2018 (2018) 3181087. <https://doi.org/10.1155/2018/3181087>.
- 897 [79] A. Folino, D.A. Zema, P.S. Calabrò, Environmental and economic sustainability of  
898 swine wastewater treatments using ammonia stripping and anaerobic digestion: A short  
899 review, *Sustain.* 12 (2020). <https://doi.org/10.3390/su12124971>.
- 900 [80] K. Xu, D. Qu, M. Zheng, X. Guo, C. Wang, Water reduction and nutrient  
901 reconcentration of hydrolyzed urine via direct-contact membrane distillation: ammonia  
902 loss and its control, *J. Environ. Eng.* 145 (2019) 04018144.  
903 [https://doi.org/10.1061/\(asce\)ee.1943-7870.0001496](https://doi.org/10.1061/(asce)ee.1943-7870.0001496).
- 904 [81] F. Tibi, J. Guo, R. Ahmad, M. Lim, M. Kim, J. Kim, Membrane distillation as post-  
905 treatment for anaerobic fluidized bed membrane bioreactor for organic and nitrogen  
906 removal, *Chemosphere*. 234 (2019) 756–762.  
907 <https://doi.org/https://doi.org/10.1016/j.chemosphere.2019.06.043>.
- 908 [82] R.R. Karri, J.N. Sahu, V. Chimmiri, Critical review of abatement of ammonia from  
909 wastewater, *J. Mol. Liq.* 261 (2018) 21–31.  
910 <https://doi.org/https://doi.org/10.1016/j.molliq.2018.03.120>.
- 911 [83] R. Sánchez-Hernández, I. Padilla, S. López-Andrés, A. López-Delgado, Al-waste-  
912 based zeolite adsorbent used for the removal of ammonium from aqueous solutions,  
913 *Int. J. Chem. Eng.* 2018 (2018) 1256197. <https://doi.org/10.1155/2018/1256197>.
- 914 [84] K. Ham, B.S. Kim, K.-Y. Choi, Enhanced ammonium removal efficiency by ion  
915 exchange process of synthetic zeolite after Na<sup>+</sup> and heat pretreatment, *Water Sci.*  
916 *Technol.* 78 (2018) 1417–1425. <https://doi.org/10.2166/wst.2018.420>.
- 917 [85] J. Desloover, A. Abate Woldeyohannis, W. Verstraete, N. Boon, K. Rabaey,  
918 Electrochemical resource recovery from digestate to prevent ammonia toxicity during  
919 anaerobic digestion, *Environ. Sci. Technol.* 46 (2012) 12209–12216.  
920 <https://doi.org/10.1021/es3028154>.
- 921 [86] A.K. Luther, J. Desloover, D.E. Fennell, K. Rabaey, Electrochemically driven  
922 extraction and recovery of ammonia from human urine, *Water Res.* 87 (2015) 367–  
923 377. <https://doi.org/10.1016/j.watres.2015.09.041>.
- 924 [87] J. de S. Oliveira Filho, S. Daguerre-Martini, M.B. Vanotti, J. Saez-Tovar, A. Rosal,  
925 M.D. Perez-Murcia, M.A. Bustamante, R. Moral, Recovery of ammonia in eaw and  
926 co-digested swine manure using gas-permeable membrane technology, *Front. Sustain.*  
927 *Food Syst.* 2 (2018) 30. <https://doi.org/10.3389/fsufs.2018.00030>.
- 928 [88] S.P. Munasinghe-Arachchige, P. Cooke, N. Nirmalakhandan, Recovery of nitrogen-  
929 fertilizer from centrate of anaerobically digested sewage sludge via gas-permeable  
930 membranes, *J. Water Process Eng.* 38 (2020) 101630.  
931 <https://doi.org/https://doi.org/10.1016/j.jwpe.2020.101630>.
- 932 [89] R.P. Ramasamy, Z. Ren, M.M. Mench, J.M. Regan, Impact of initial biofilm growth  
933 on the anode impedance of microbial fuel cells, *Biotechnol Bioeng.* 101 (2008) 101–  
934 108. <https://doi.org/10.1002/bit.21878>.
- 935